Multimessanger Astronomy with Gravitational Waves and Electromagnetic Signals

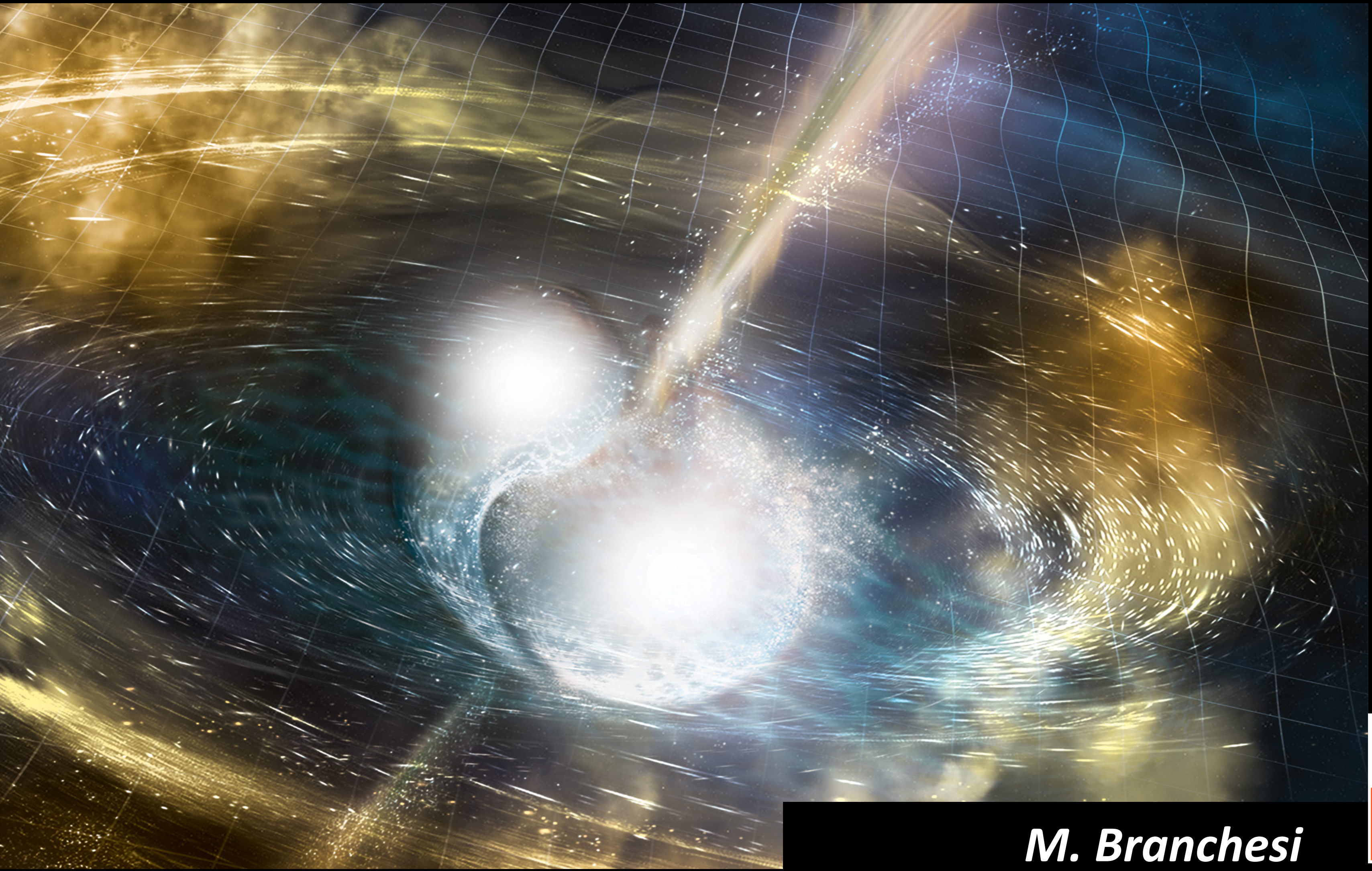

M. Branchesi
Gran Sasso Science Institute
INFN/LNGS and INAF

Radioactively powered transients

Relativistic astrophysics

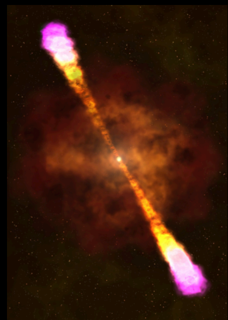

Nucleosynthesis and enrichment of the Universe

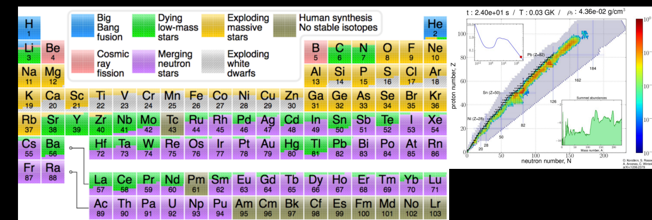

Compact object formation and evolution

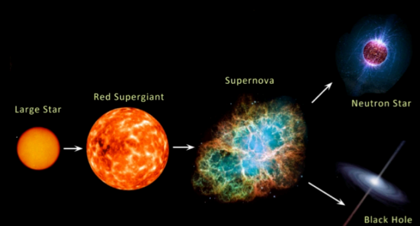

Cosmology

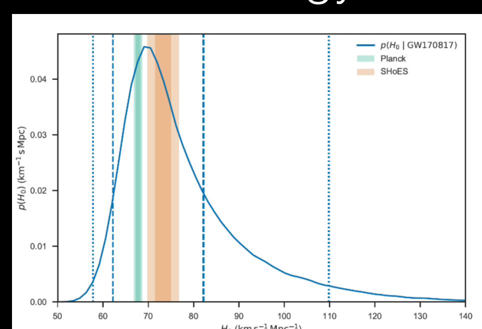

Nuclear matter physics

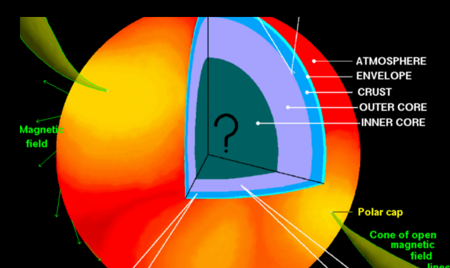

A new window into the Universe

Credit: LIGO–Virgo

ASTROPHYSICAL SOURCES emitting transient GW signals detectable by LIGO and Virgo (10-1000 Hz)

Coalescence of binary system of neutron stars and/or stellar-mass black-hole

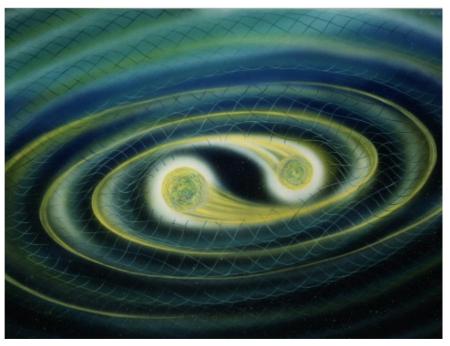

- Orbital evolution and GW signals accurately modeled by post-Newtonian approximation and numerical simulations
  → precise waveforms
- **Energy emitted in GWs (BNS): ~$10^{-2} M_o c^2$**

Isolated neutron-star instabilities

Core-collapse of massive stars

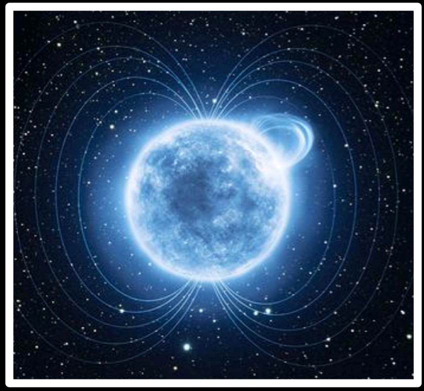

- Modeling of the GW shape and strength is complicated → **uncertain waveforms**
- **Energy emitted in GWs:**

~ $10^{-9} M_o c^2$ for the core-collapse

~10^{-16} – $10^{-6} M_o c^2$ for isolated NSs

ASTROPHYSICAL SOURCES emitting transient GW signals detectable by LIGO and Virgo (10-1000 Hz)

Coalescence of binary system of neutron stars and/or stellar-mass black-hole

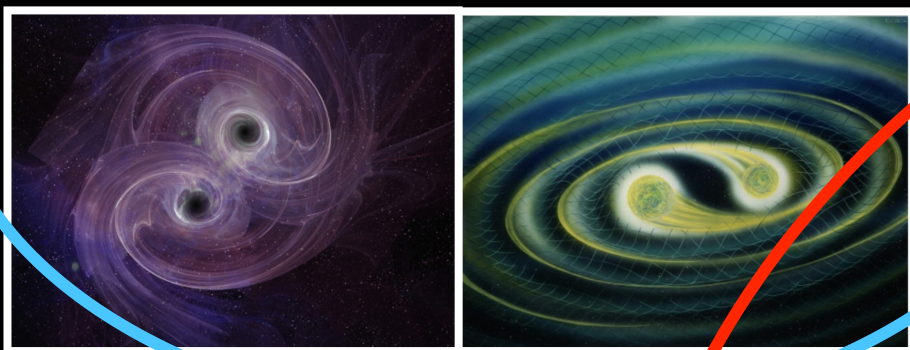

→ MATCHED-FILTER MODEL SEARCHES

Core-collapse of massive stars

Isolated neutron-star instabilities

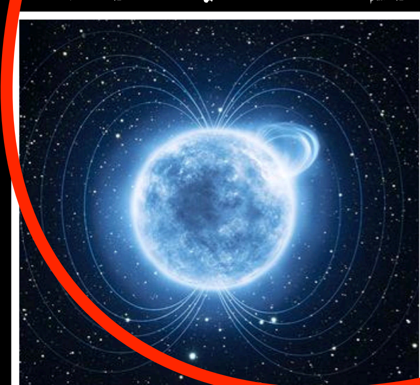

UNMODELED SEARCHES

Modelled compact binary coalescence searches

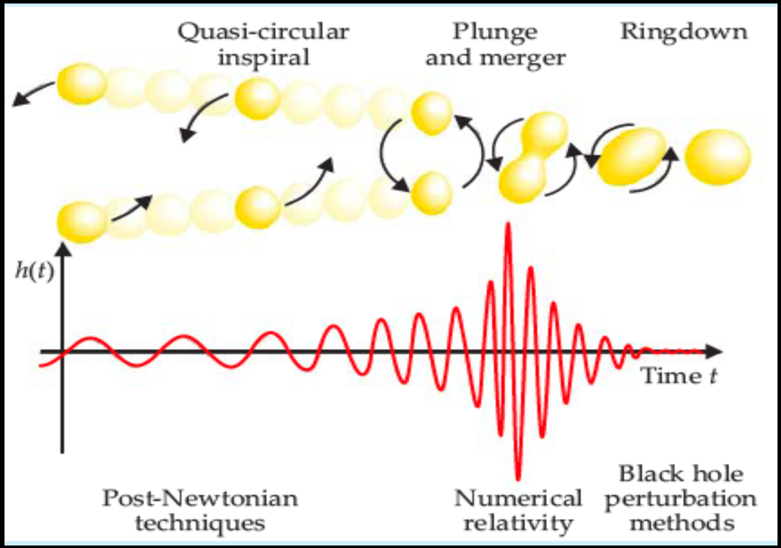

Waveforms depend on

- ***intrinsic parameters**: **masses** and **spins** of the binary system (plus eccentricity, NS compactness, tidal deformability)*
- ***extrinsic parameters** that describe location, distance, merger time and system orientation with respect to an observer*

Detection phase: known waveforms → **MATCHED FILTERING**

- Using waveform templates for a range of intrinsic parameters (masses and spin)
- "Extrinsic" parameters absorbed in overall amplitude

After detection → ***Source PARAMETER RECONSTRUCTION:***

- Algorithms to explore the full-parameter space and find most likely values for sky location, masses, distance, orientation, spin…

Matched filtering searches

Template bank

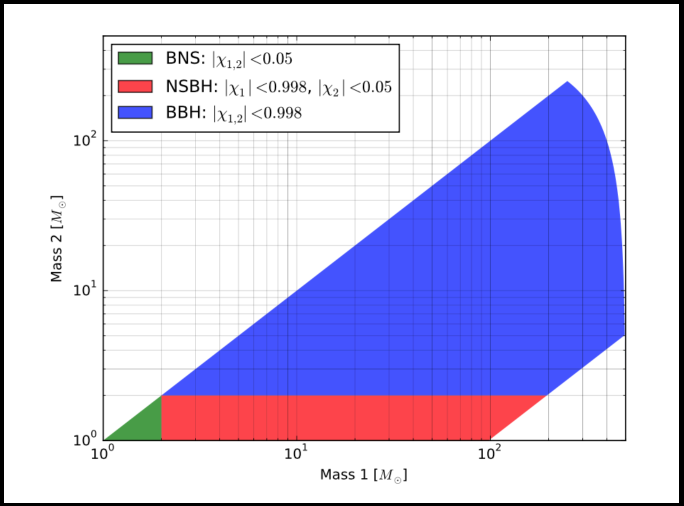

LVC Phys. Rev. X 6 (2016)

TEMPLATE

OBSERVATIONS

$$\langle h|s\rangle(t) = 4\Re \int_0^\infty \frac{\tilde{h}^*(f)\tilde{s}(f)e^{2\pi i f t}}{S_\mathrm{n}(f)} df$$

NOISE MODEL

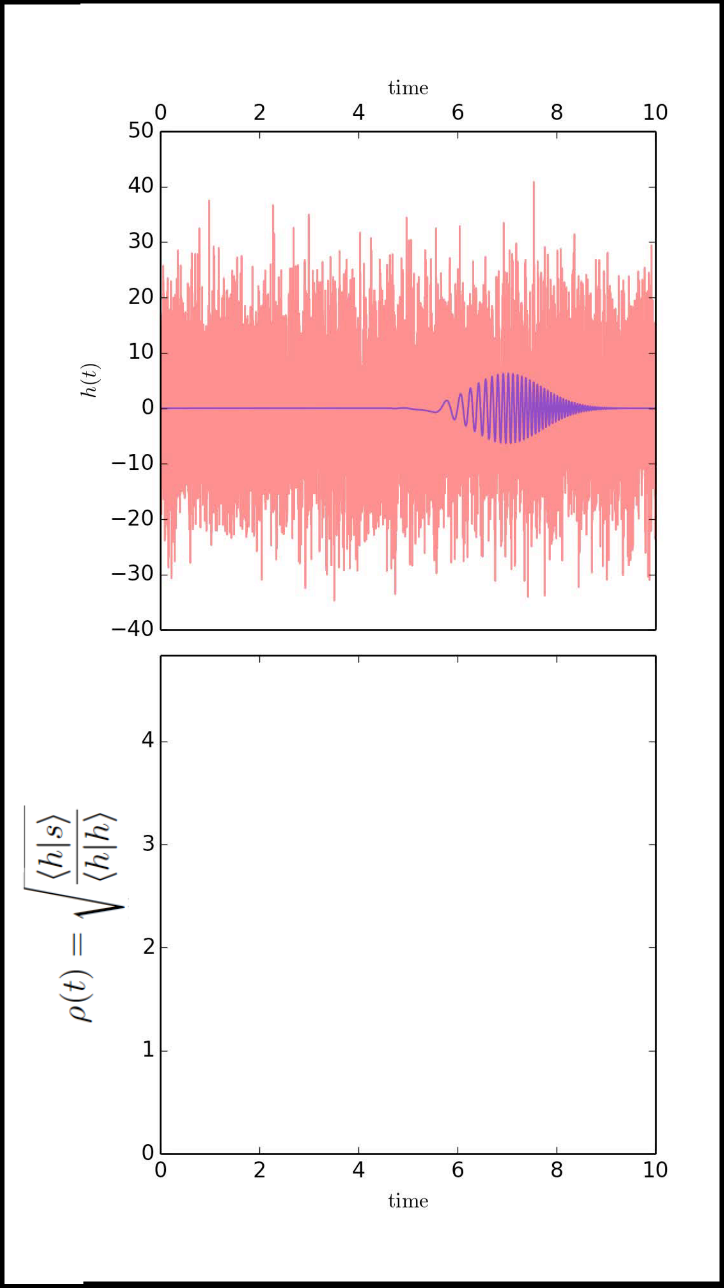

Unmodeled GW transient searches

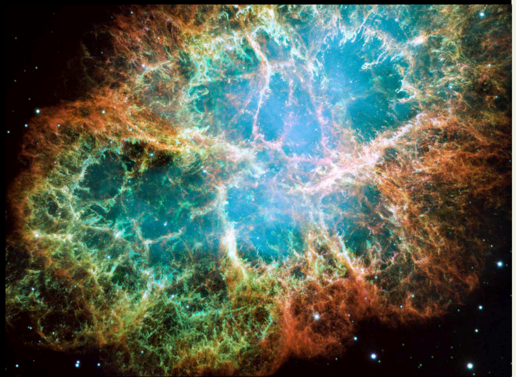

Transient sources:
- Core-collapse of massive stars
- Cosmic strings
- Neutron star instabilities
- Intermediate Massive BH
- ... the unknown

Poorly modelled
→ Can't use matched filtering

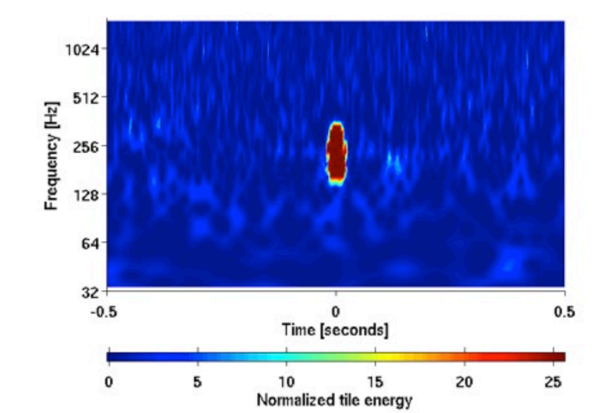

Detection without unknown waveform
→ **LOOK FOR "EXCESS POWER"**

All-sky, all-time search for transient as increase in power (hot pixels) in time-frequency map, minimal assumptions:

1. Duration: 1 ms to 1 s (characteristic time scale for stellar mass objects) → now also to a few hundreds of sec
2. Frequency: 10 to 5000 Hz (determined by detector's sensitivity)
3. **Signal appears coherently** in multiple detectors, consistent with antenna pattern → coincidence, coherent statistics, sky location

Noise fluctuations can be eliminated based on their non-correlation between detectors

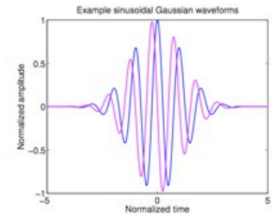

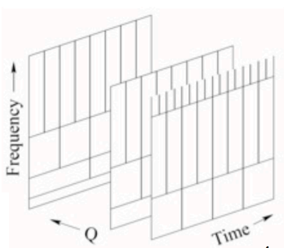

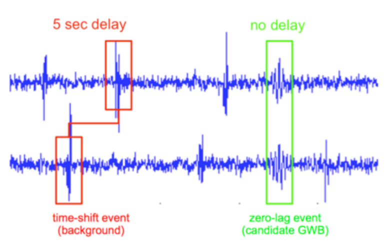

4

Low-latency GW data analysis pipelines to promptly identify GW candidates and send GW alerts

GW candidates

Sky Localization

EM facilities

LIGO-H LIGO-L

Virgo

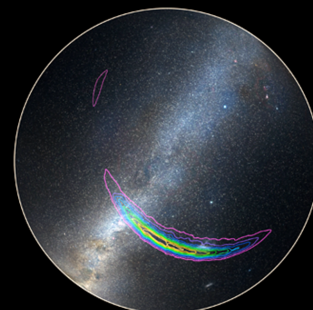

Event validation

Low-latency search
to identify the GW-candidates

Software to

- select statistically significant triggers wrt background
- check detector sanity and data quality
- determine source localization

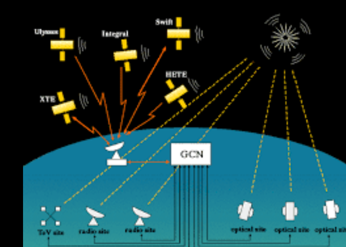

a few min → **30 min**

O1, O2 run

LVC 2019, ApJ, 875, 161

O3 run started in April

GW candidates

Sky Localization

EM facilities

LIGO-H LIGO-L

Virgo

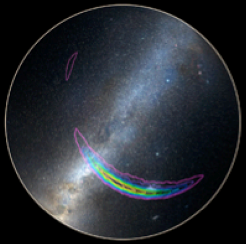

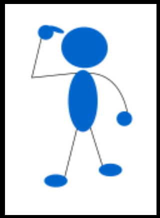

Event validation

RETRACTION

or

CONFIRMATION

GCN

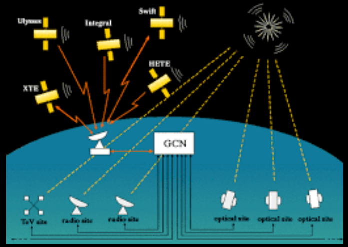

within min → 30 min- few hrs

Parameter estimation codes → Hours,days → GW candidate updates

What is important to know to set-up the EM counterpart search?

Strain sensitivities as a function of frequency

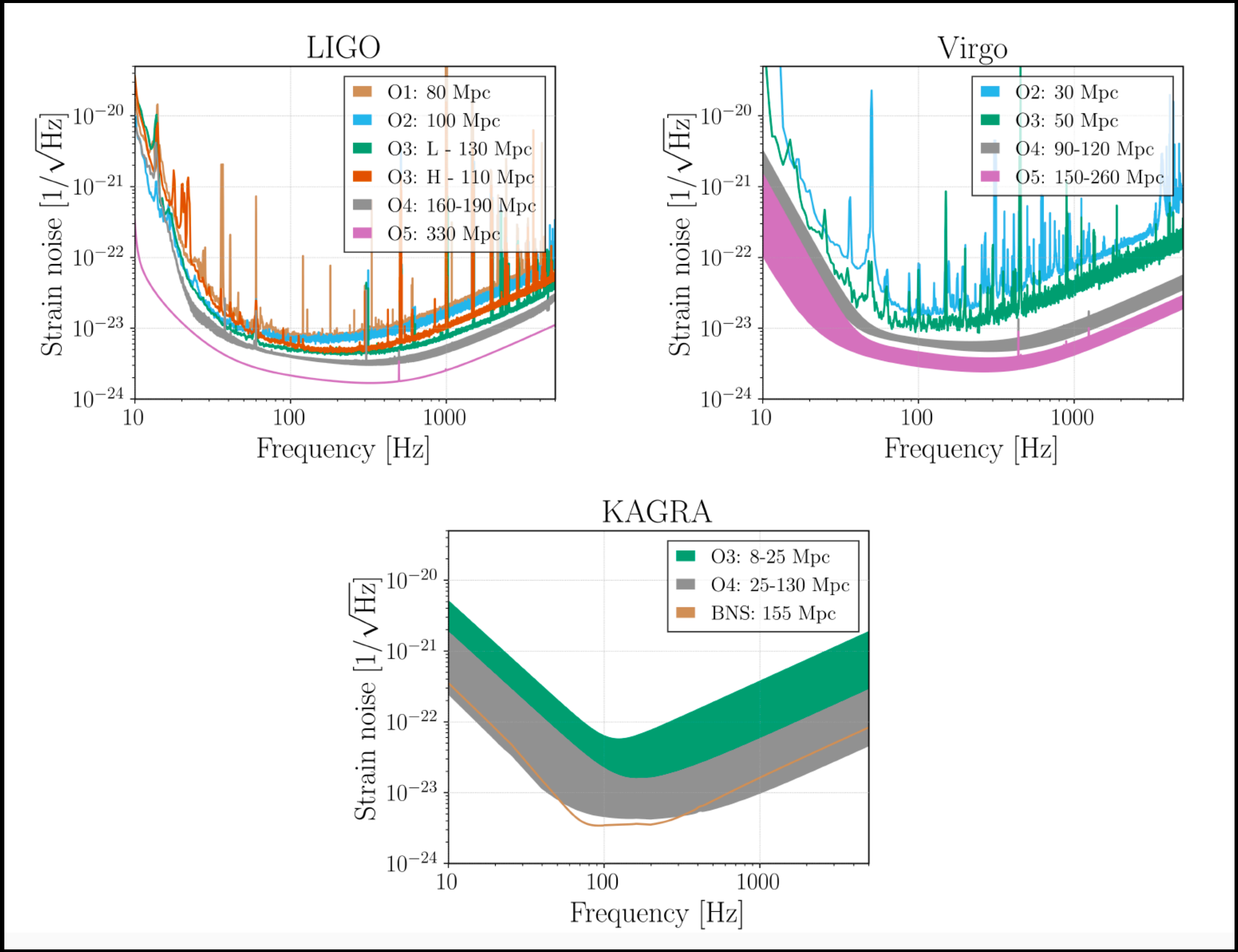

Abbott et al. 2020, LRR

SENSITIVITY IN TERMS OF RANGE/HORIZON DISTANCE

- Range: the volume- and orientation-averaged distance at which a compact binary coalescence gives a matched filter SNR of 8 in a single detector

- Distance for face-on system: distance at which an optimally oriented system (orbital plane perpendicular to the line of sight) would be observed with an SNR of 8: range x 1.5

- Horizon: distance at which an optimally oriented and located binary system would be observed with an SNR of 8: range x 2.26

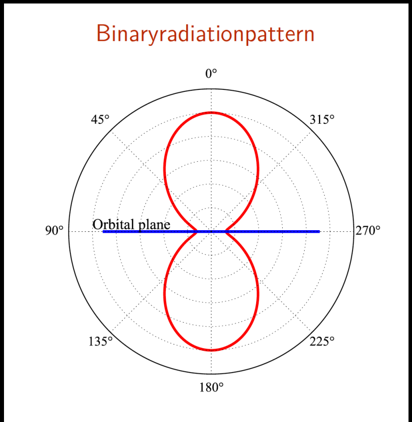

RANGES corresponding to the orientation-averaged spacetime volumes surveyed per unit detector time

SNR = 8 in each detector

		O1	O2	O3	O4	O5
BNS Range (Mpc) 1.4 Mo+1.4 Mo	aLIGO	80	100	110 – 130	160 – 190	330
	AdV	-	30	50	90 – 120	150 – 260
	KAGRA	-	-	8 – 25	25 – 130	130+
BBH Range (Mpc) 30 Mo+30 Mo	aLIGO	740	910	990 – 1200	1400 – 1600	2500
	AdV	-	270	500	860 – 1100	1300 – 2100
	KAGRA	-	-	80 – 260	260 – 1200	1200+
NSBH Range (Mpc) 1.4 Mo+10 Mo	aLIGO	140	180	190 – 240	300 – 330	590
	AdV	-	50	90	170 – 220	270 – 480
	KAGRA	-	-	15 – 45	45 – 290	290+
Burst Range (Mpc) [$E_{GW} = 10^{-2} M_\odot c^2$]	aLIGO	50	60	80 – 90	110 – 120	210
	AdV	-	25	35	65 – 80	100 – 155
	KAGRA	-	-	5 – 25	25 – 95	95+
Burst Range (kpc) [$E_{GW} = 10^{-9} M_\odot c^2$]	aLIGO	15	20	25 – 30	35 – 40	70
	AdV	-	10	10	20 – 25	35 – 50
	KAGRA	-	-	0 – 10	10 – 30	30+

LVK arXiv:1304.0670

Sky location - single GW detector directional sensitivity

$$\frac{\Delta L}{L} = h_{\text{det}}(t) = F_+ h_+(t) + F_x h_x(t)$$

The **antenna pattern** depends on the polarization in a certain (x,+) basis

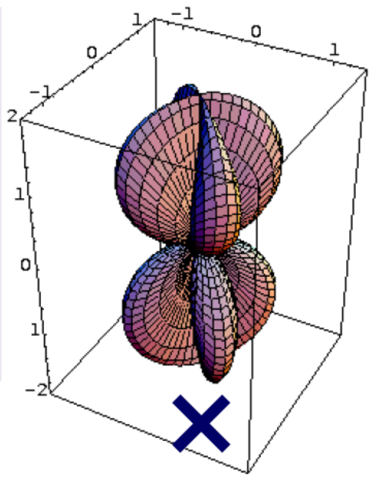

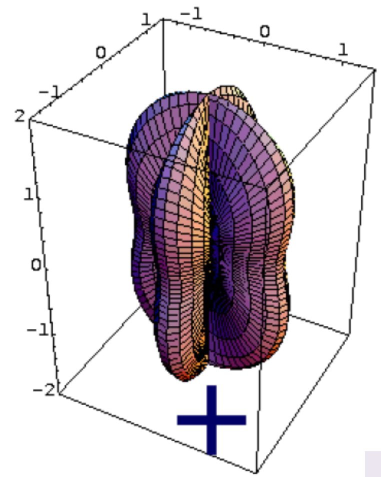

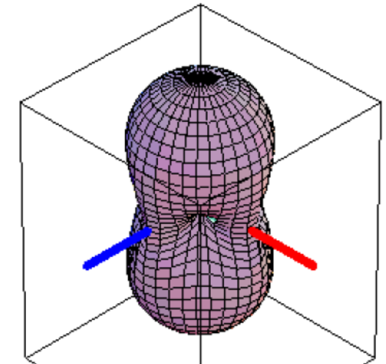

RMS sensitivity

$$\sqrt{F_+(\theta,\phi)^2 + F_x(\theta,\phi)^2}$$

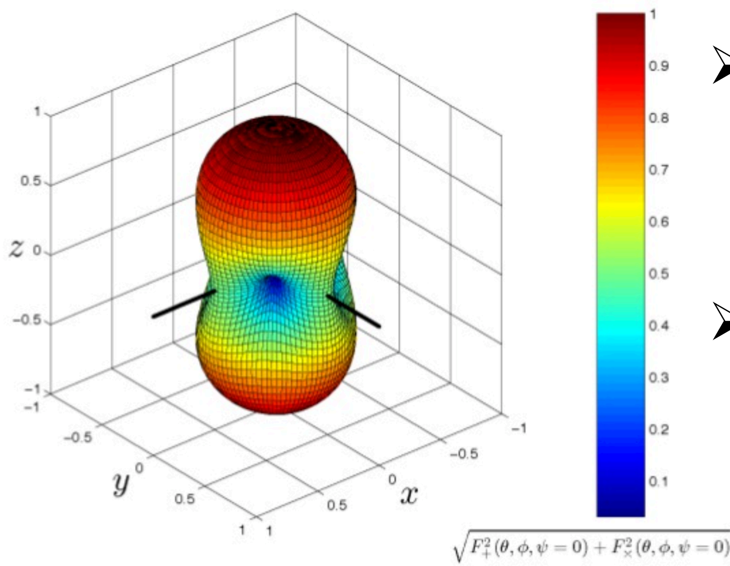

- Single GW detector is a **good all-sky monitor**, nearly omni-directional (the transparency of Earth to GWs)
- But does not have good directional sensitivity, **not a pointing instrument!** It has a very poor angular resolution (about 100 deg)

The source localization requires a network of GW detectors

*The **sky position** of a GW source is mainly **evaluated by triangulation**, measuring the differences in signal arrival times at the different network detector sites*

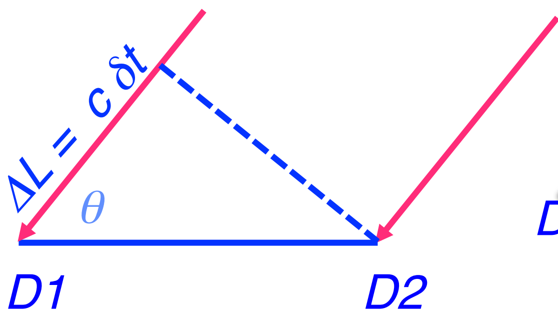

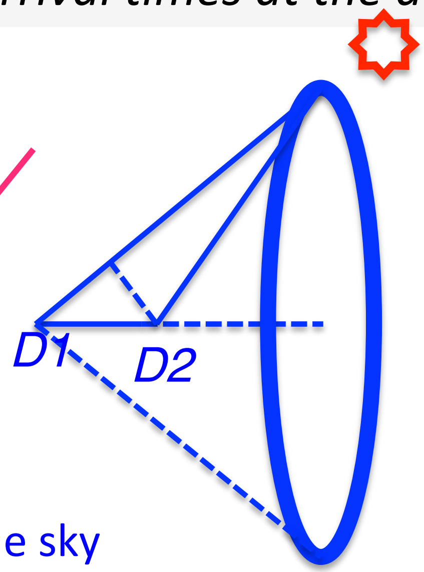

2-detectors → annulus in the sky

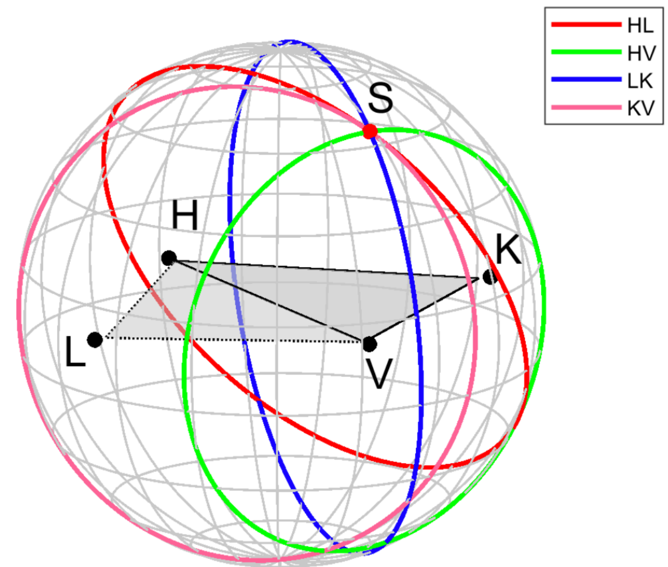

4-detectors → localize

The localization capabilty improves with signal SNR → the sky localization area scales inversely with the square of the SNR

Compact binary Coalescence (CBC) Sky localization map

Arrival time Amplitudes Phase

→ sky location
→ distance to the source
→ binary orientation

Sky location also in 3 D

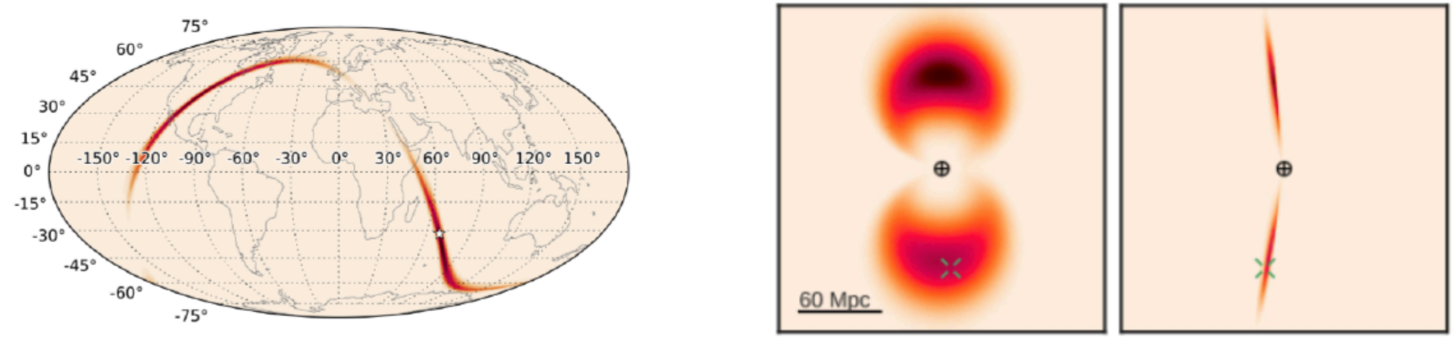

Sky direction

Projections of 3d location

Online pipelines estimate → arrival time, phase, signal amplitude at each detector

These estimates + template masses : constrain direction of GW arrival and distance to the source

→ **BAYESTAR** **(Singer et al 2014, ApJ, 795, 2016 ApJL, 829)**: estimate 3D location in <1 minute

→ **LALInference**, **full PE Bayesian MCMC** **(Veitch 2015; Berry et al. 2015),** modeling the inspiral-merger-ring down phase and taking into account the calibration uncertainty

2017 August 14, 10:30:43 UT

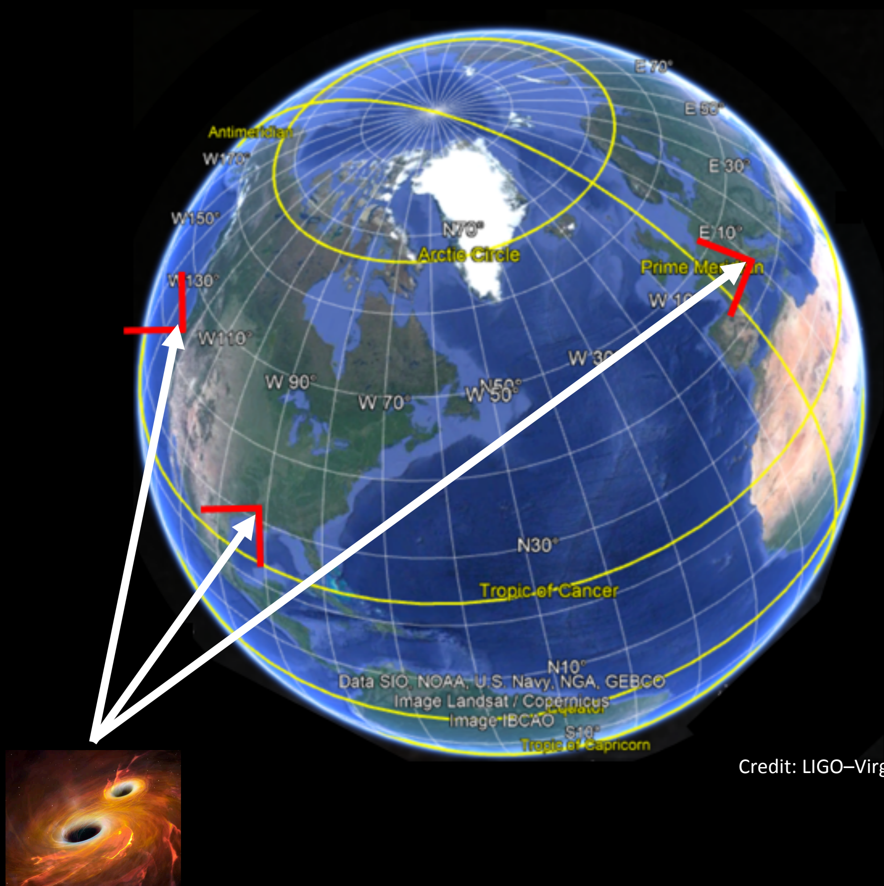

Credit: LIGO–Virgo

Virgo observed its first BBH coalescence, GW170814

2017 August 14

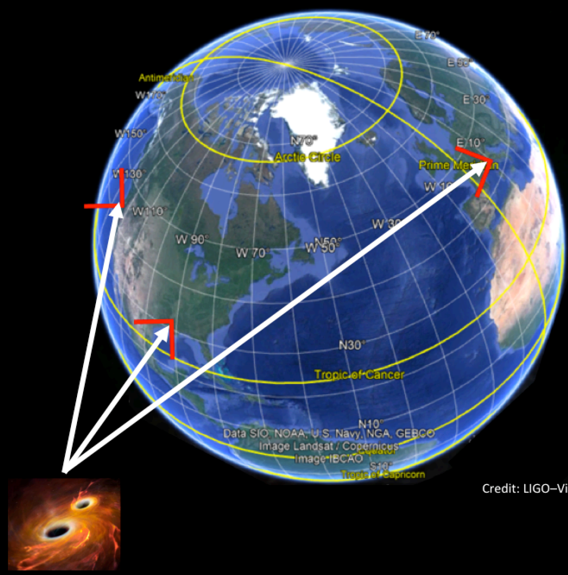

Credit: LIGO–Virgo

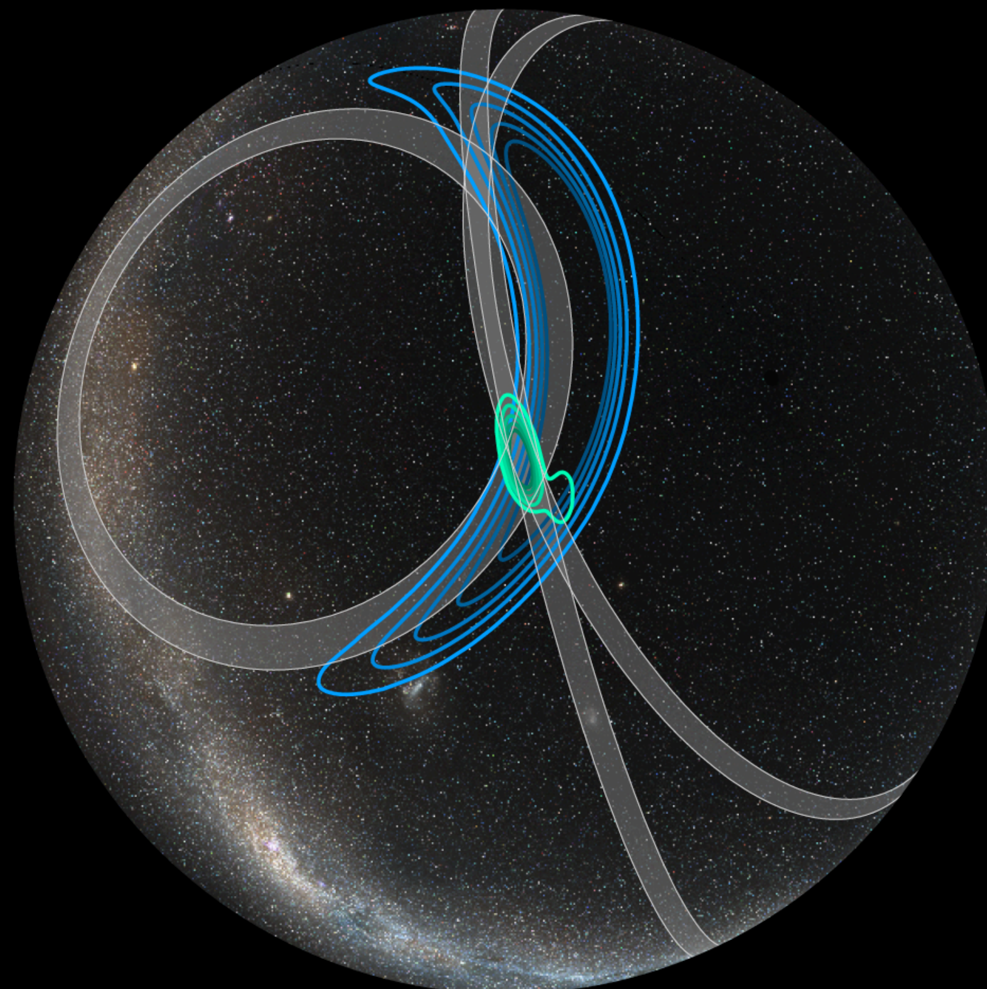

Credit: Leo Singer

2017 August 14

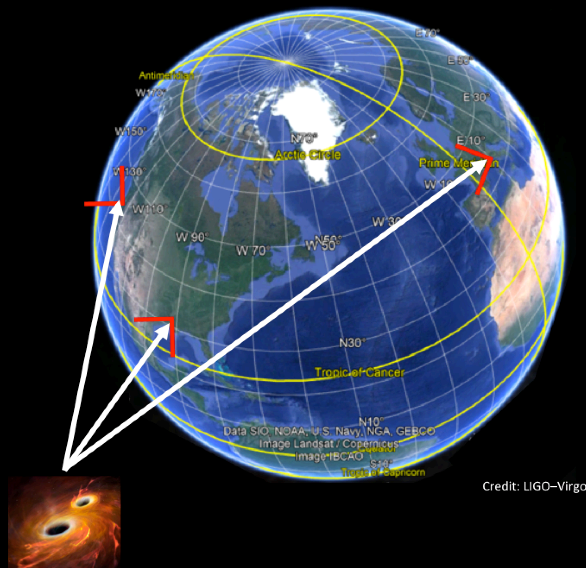

Credit: LIGO–Virgo

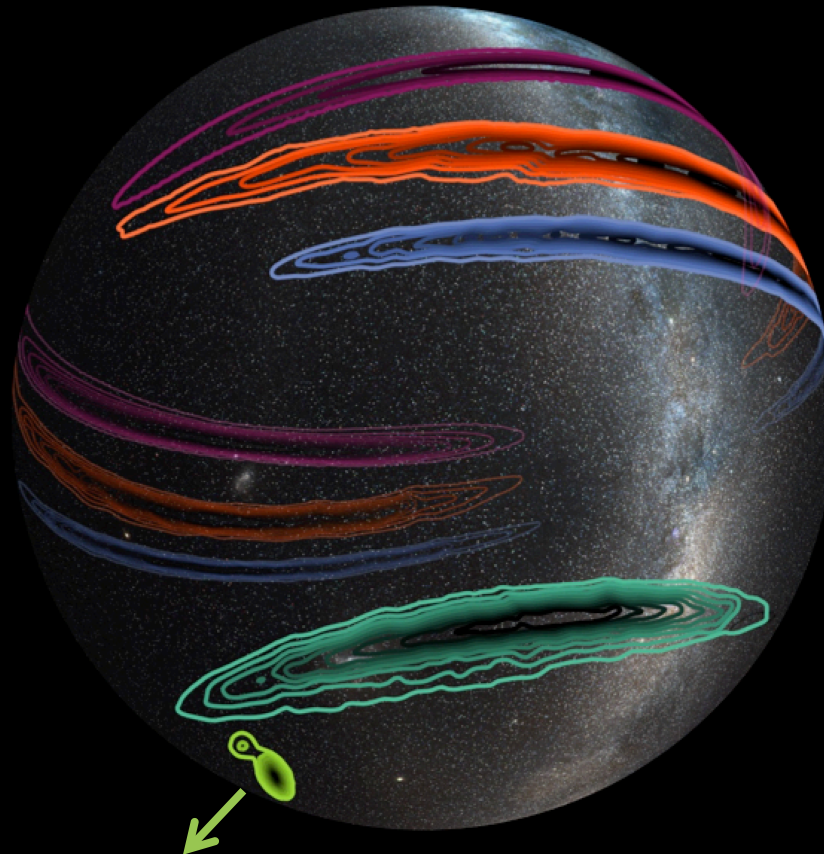

GW170814

Credit: LIGO/Virgo/NASA/Leo Singer
(Milky Way image: Axel Mellinger)

LH 1160 square degrees

LHV 60 square degrees

Hunt the elusive EM-counterpart!

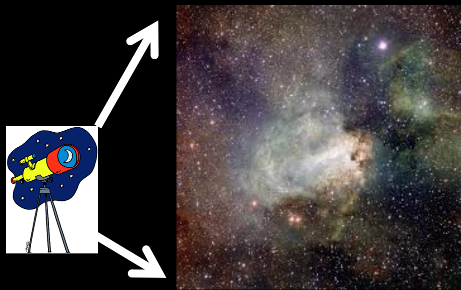

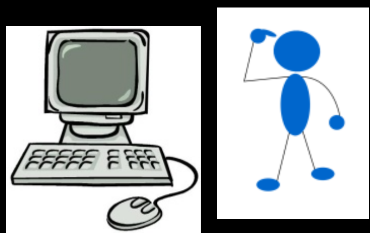

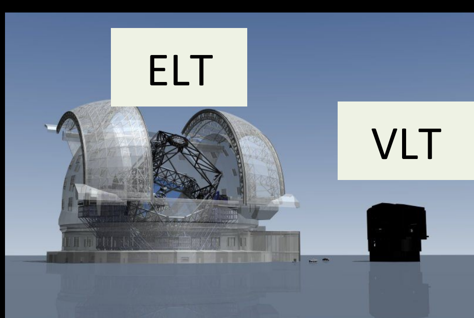

Wide-field telescope
FOV >1 sq.degree

"Fast" and "smart" software to select a sample of candidate counterparts

Larger telescope to **characterize** the candidate nature

The EM Counterpart!

to cover hundreds/thousands of square degrees

to remove transients contaminants

To obtain observational time for the characterization

Hunt the elusive EM-counterpart!

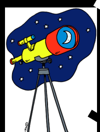


Wide-field telescope
FOV >1 sq.degree

to cover hundreds/thousands of square degrees


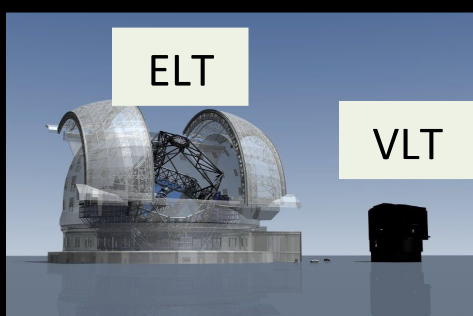

Galaxy-targeting observational strategy

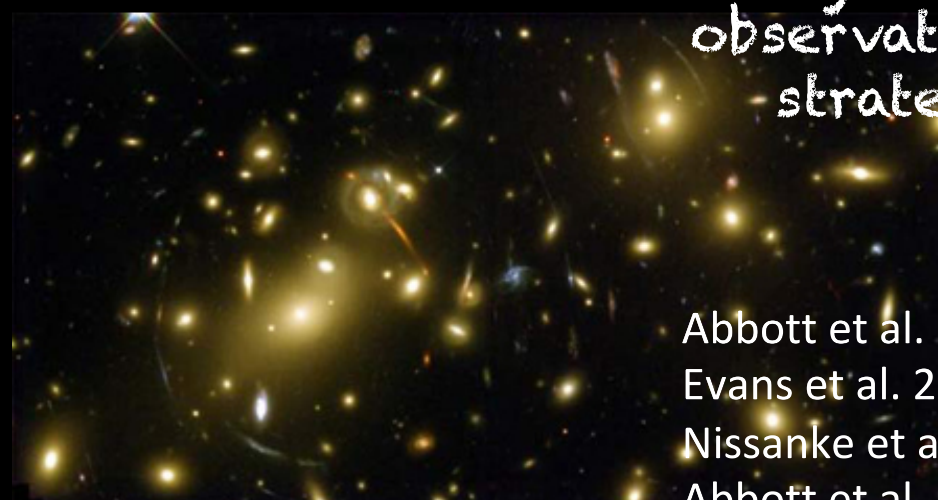

Abbott et al. 2012 A&A
Evans et al. 2012
Nissanke et al. 2013
Abbott et al. 2014 ApJS
Gehrels et al. 2016

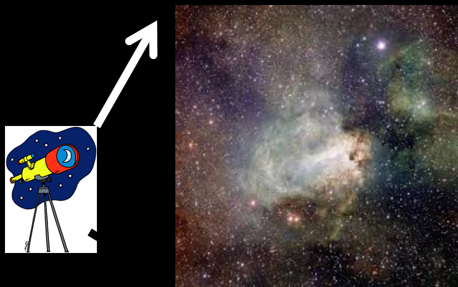

Wide-field telescope
FOV >1 sq.degree

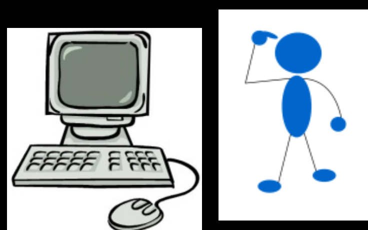

“Fast” and “smart” software to select a sample of candidate counterparts

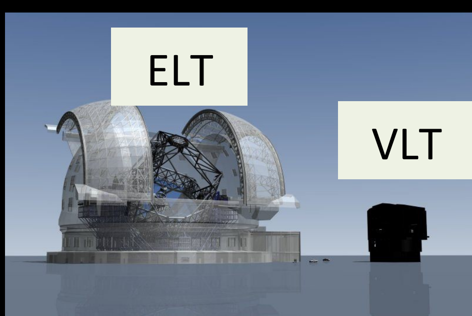

Larger telescope to **characterize** the candidate nature

Optical/NIR band

10^4-10^5 variable objects over 100 sq. degrees

Artifacts and many astrophysical contaminants

M-dwarf flares (min to hrs)
3 (0.3) deg^{-2} up to red mag 24
at 20 (80) deg latitude
(Ridgway et al., 2014)

Supernovae (days to month)
7 deg^{-2} up to red mag 24
(Graur et al., 2014; Dahlen et al., 2012; Cappellaro, 2014)

A few tens of candidate counterparts

Hunt the elusive EM-counterpart!

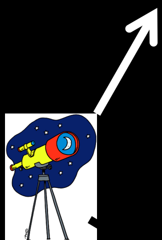


Wide-field telescope
FOV >1 sq.degree


“Fast” and “smart” software to select a sample of candidate counterparts

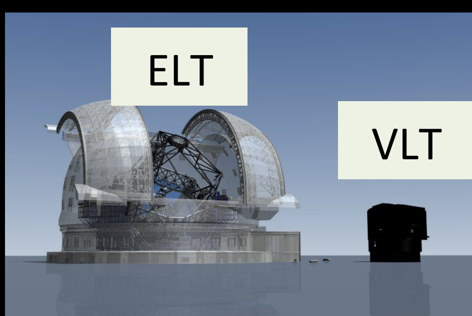

Larger telescope to **characterize** the candidate nature

X-rays

✓ less contaminants

Transient rate **2.5 x 10^{-3} deg^{-2}**
flux$_{0.2\text{-}2KeV}$ > 3 x 10^{-12}ergs^{-1}cm^{-2}
(Kanner et al. 2013)

x no wide-field telescope

Gamma-rays

✓ less contaminants
✓ all-sky monitors
x beamed emission

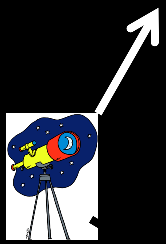

Wide-field telescope
FOV >1 sq.degree

"Fast" and "smart" software to select a sample of candidate counterparts

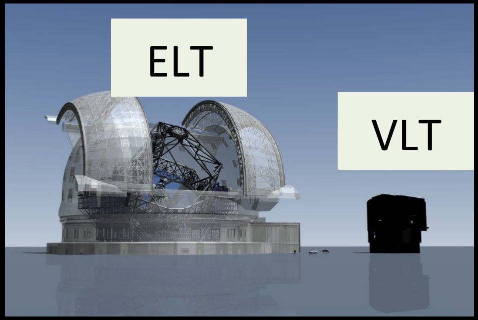

Larger telescope to **characterize** the candidate nature

The EM Counterpart!

Radio

✓ less contaminants

Transient rate < 0.37 deg^{-2}
peak-flux_1.4 GHz > 0.21 mJy
timescales 1 d – 3 m
(Mooley et al., 2013)

✓ wide-field array at low frequencies (MHz)

x faint sources

x long delay GW → radio emission

What can help to define an observational strategy?

ALERT CONTENTS to support observing startegy

- Estimate of FALSE ALARM RATE (FAR) of the event candidate
  FAR=Rate of noise events louder than the candidate event

- Event TIME and LOCALIZATION given as a posterior probability distribution of the source's sky position(HEALPix FITS file)

For CBC candidates:

- 3-D skymap (Singer et al. 2016, ApJL 829, L15), with direction dependent luminosity distance
- Luminosity distance marginalized over whole sky
  (mean+/-standard deviation)

ALERT CONTENTS

- For CBC candidates, CLASSIFICATION and PROPERTIES

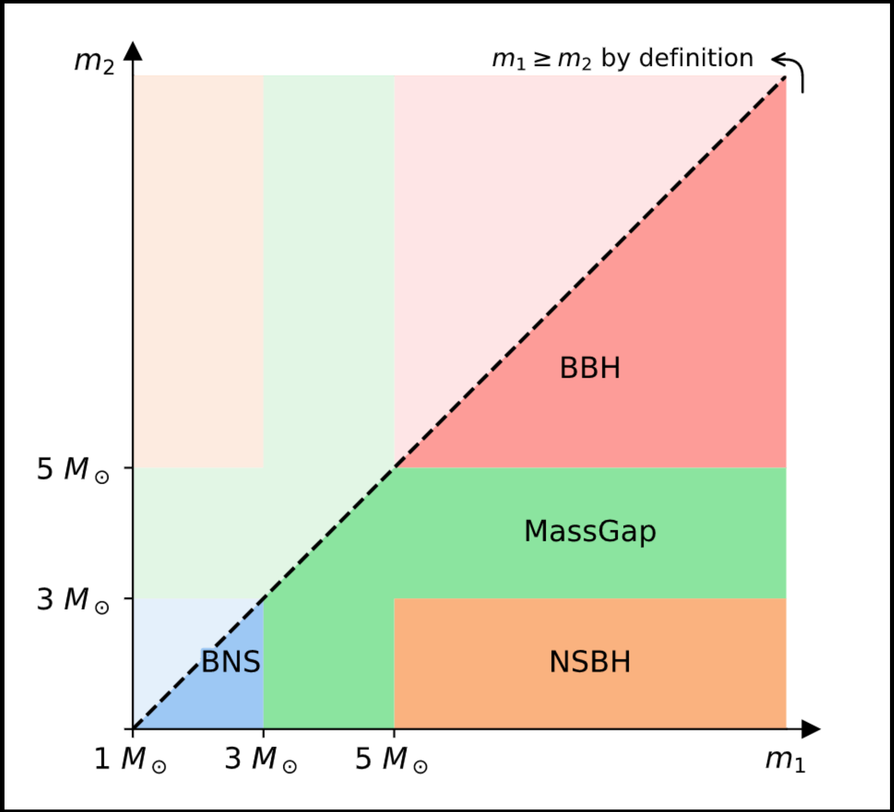

Credit: User Guide

Categories in terms of component masses

CLASSIFICATION:

→ P_astro probability that the signal is astrophyiscal

This probability evaluates whether the source belongs to one of five categories: BNS, mass gap, NSBH, BBH, Terrestrial

Based on our knowledge of trigger distribution, assumptions about signal distribution (such as that sources are uniformly distributed involume), and knowledge and assumptions about merger rate per unit volume fo reach class of sources

(See Kapadia et al 2019)

PROPERTIES

- HasNS → probability that the mass of one or more of the binary's two companion compact objects is consistent with a neutron star.

- **HasRemnant** → probability that a non-zero amount of neutron star material remained outside the final remnant compact object (a necessary but not sufficient condition to produce certain kinds of electromagnetic emission such as a short GR or a kilonova)

(Foucart 2012, 2018, PhRvD, Pannarale & Ohme, 2014, ApJ)

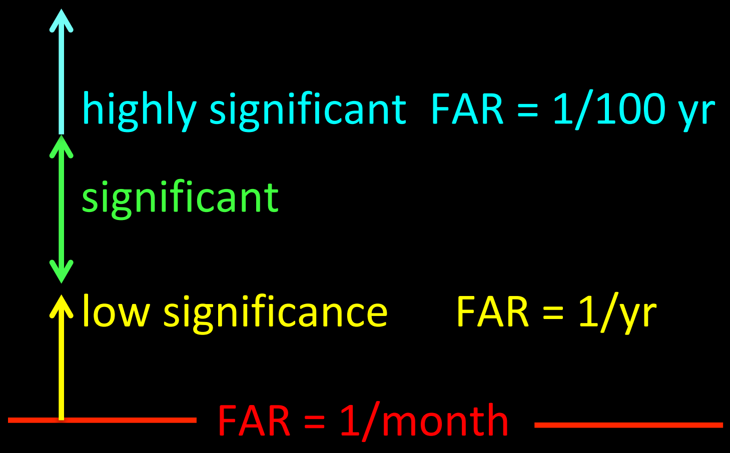

FAR = Rate of noise events louder than the candidate event

Candidates to be observed selected based on the observer's choice of FAR threshold highly significant FAR = 1/100 yr

significant

low significance FAR = 1/yr

FAR = 1/month

→ FAR = Rate of noise events louder than the candidate event

↓

Candidates to be observed selected based on the observer's choice of FAR threshold

→ Sky map + basic source classification

Credit: G. Greco, GWsky https://github.com/ggreco77/GWsky

→ To decide the search type

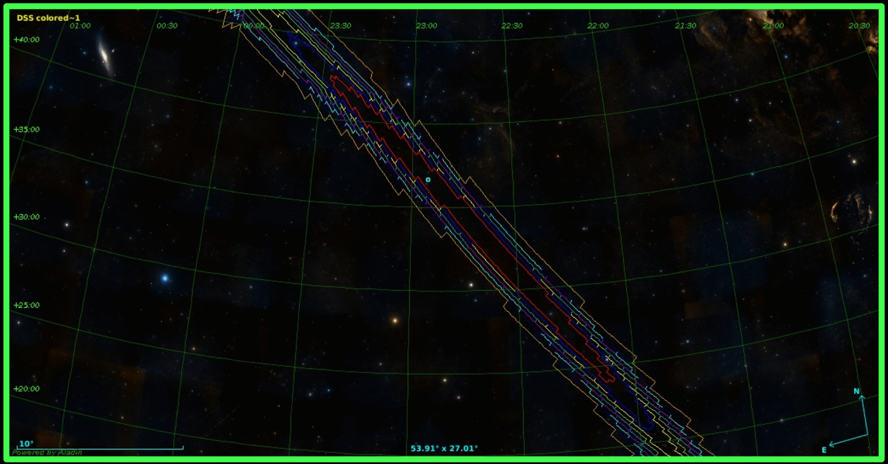

Tiling the sky map to maximize the enclosed localization probability

DES, Annis et al. 2016, ApJL

Burst → failed-SNe

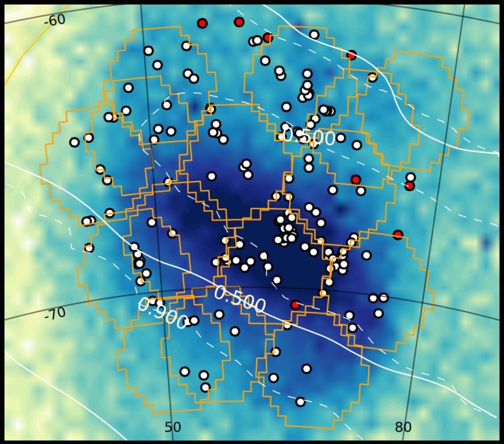

Search for missing Supergiants in the LMC

Sky map + source classification + distance

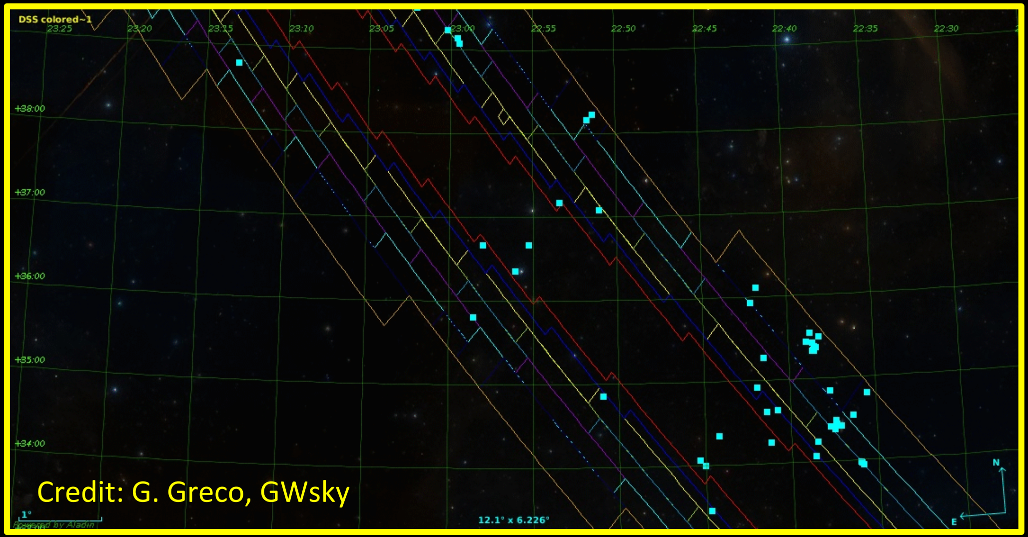

Targeting ranked galaxies

(Small FoV instruments)

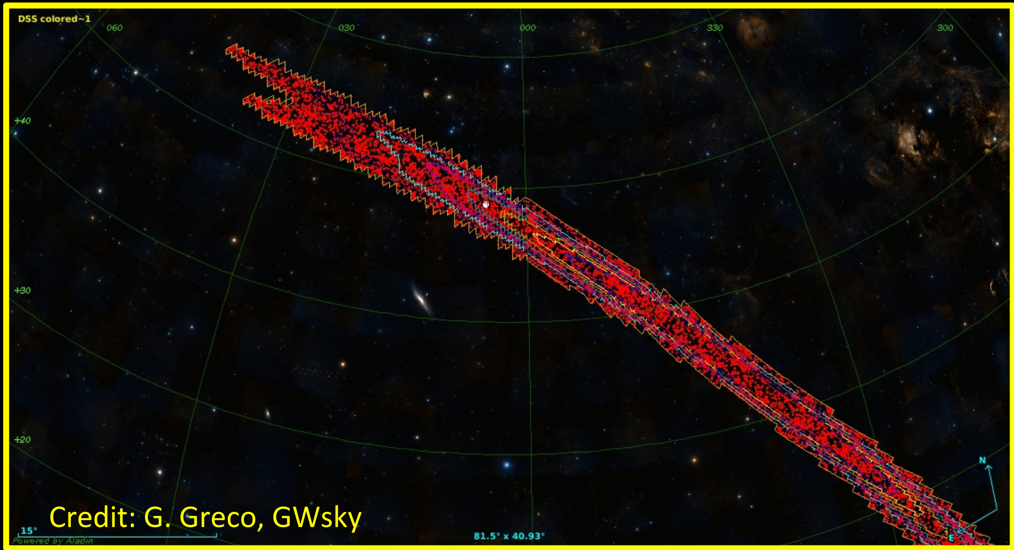

Targeting ranked FoV pointings

(Instruments FoV > 1 deg^2)

Sky map weighted by galaxy luminosity

For each FoV →

$$P = \sum \frac{L_i}{L_{tot}} P_{GW}$$

P_{GW} = probability that GW candidate lies within the FoV

See e.g Evans et al. 2016, MNRAS

HOW TO RANK THE GALAXIES?

From theoretical simulations: identify the most probable host
by combining the results of population-synthesis models together with galaxy catalogs from galaxy cosmological simulation

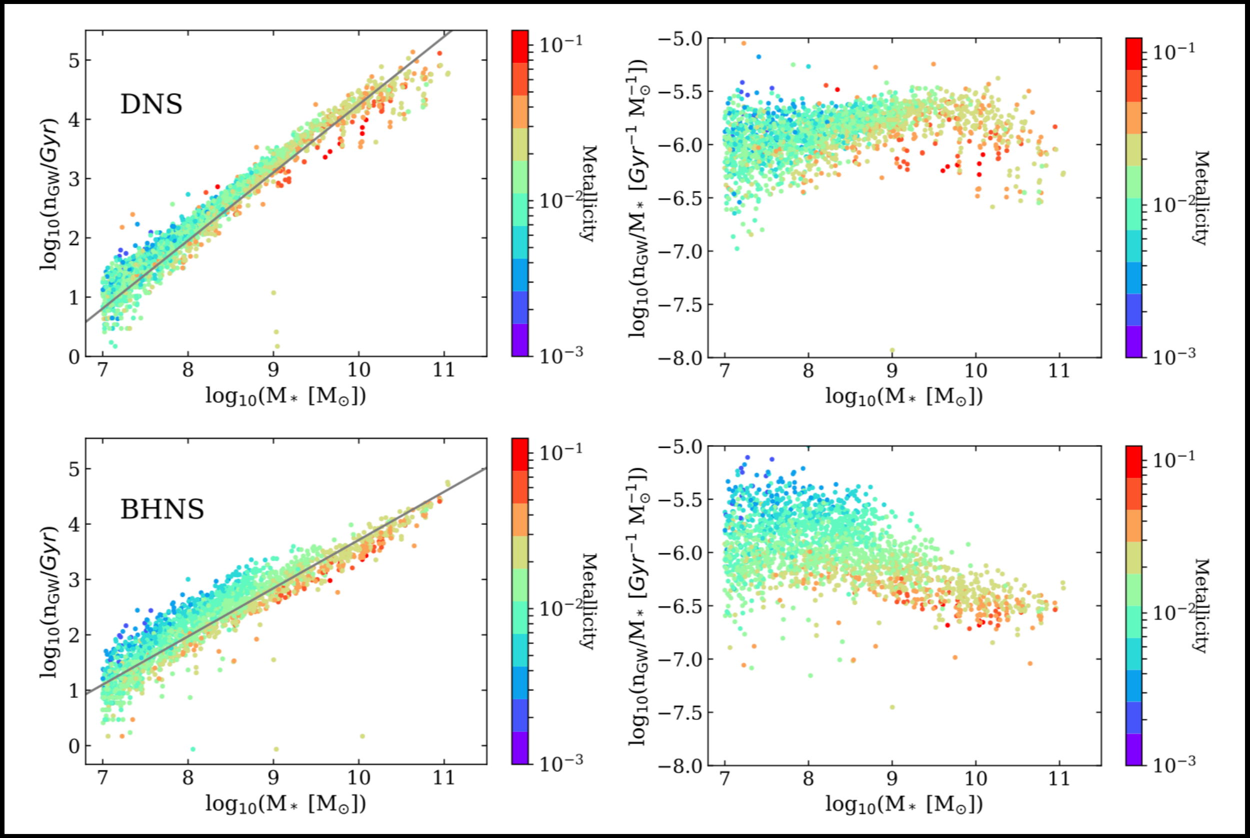

Artale et al. 2019 MNRAS

- strong correlation between host galaxy mass and merger rate
- low mass galaxies have a more efficient merger rate per galaxy of NSBH systems

REAL OBSERVATIONS → GALAXY CATALOG + 3D SKY LOCALIZATION MAP

The overall probability of the merger occurring in a galaxy is given by

1) Localization probability

$$P_{loc} = P_{(RA,DEC)} P_{(D_l)}$$

$$\Rightarrow P = P_{loc} P_{lum}$$

2) Mass/SFR probability

$$P_{lum} = \frac{L_{K,B}}{L_{tot}} = \frac{L_{K,B}}{\sum L_{K,B}}$$

After the observations the same formalism is used to evaluate the probability covered by the galaxy targeted search (including catalog incompleteness)

See e.g. Gehrels et al. 2016, Arcavi et al. 2017, Salmon 2019

Electromagnetic emissions from gravitational wave sources detectable by ground-based detectors (10-1000 Hz)

ASTROPHYSICAL SOURCES emitting transient GW signals detectable by LIGO and Virgo (10-1000 Hz)

Coalescence of binary system of neutron stars and/or stellar-mass black-hole

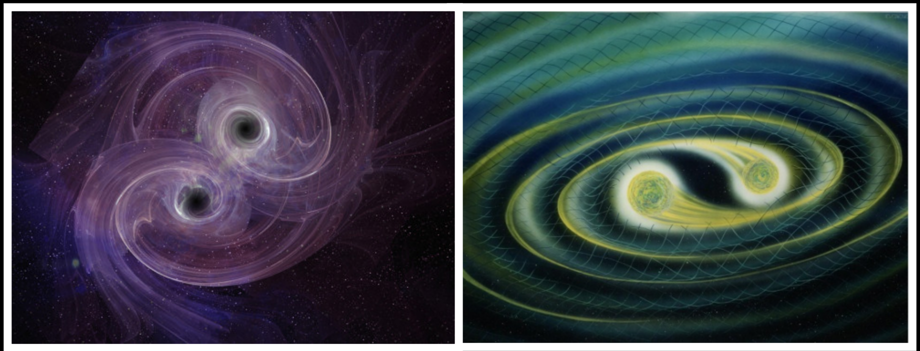

Core-collapse of massive stars

Isolated NSs instabilties

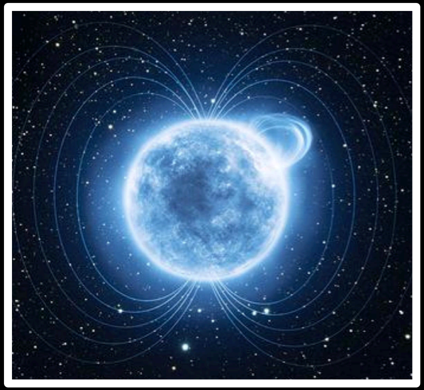

EM emissions

NS-NS and NS-BH mergers

Short Gamma Ray Burst (sGRB)

Ultra-relativistic outflow

Beamed emission

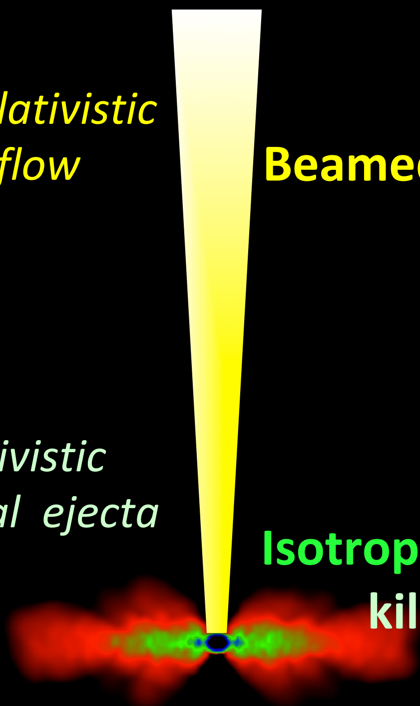

Sub-relativistic dynamical ejecta

Isotropic emission

kilonova

disk wind outflow

spin-down luminosity

Core-collapse of massive stars

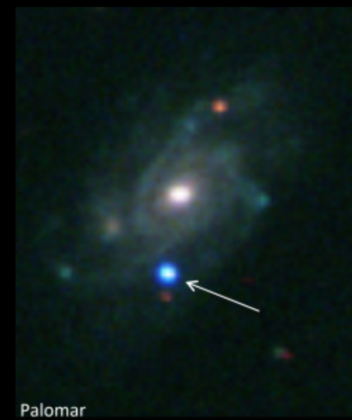

SBO X-ray/UV

Optical

Radio

+ Long GRB

Isolated NS instabilities

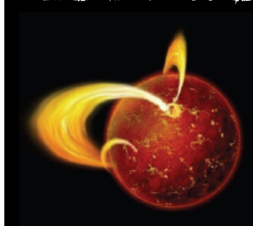

Soft Gamma Ray Repeaters and Anomalous X-ray Pulsars

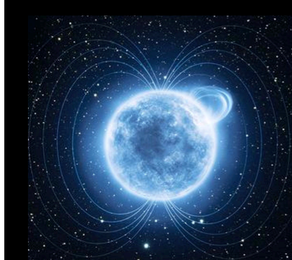

Radio/gamma-ray Pulsar glitches

NS-NS and NS-BH inspiral and merger

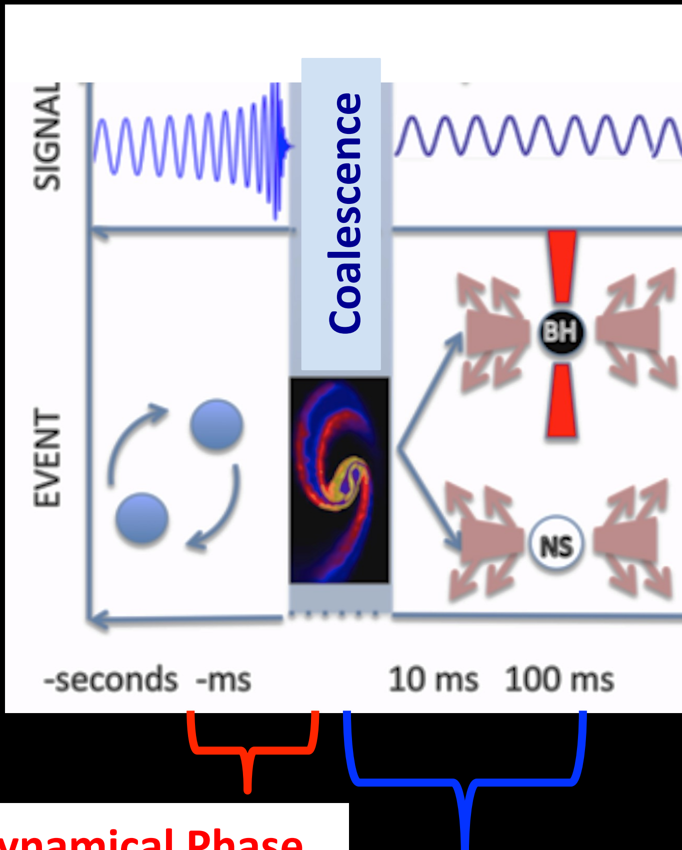

Dynamical Phase

Accretion phase

Fernandez & Metzger 2016, ARNPS, 66

The merger gives rise to:

- dynamically ejected unbound mass
- ejected mass gravitationally bound to the central remnant either falls back or circularizes into an accretion disk

NS-NS binary → <u>**unbound mass**</u> **of 10^{-4} -10^{-2} Mo ejected at 0.1-0.3c,** which depends on **total mass, mass ratio, EOS NS and binary eccentricity**

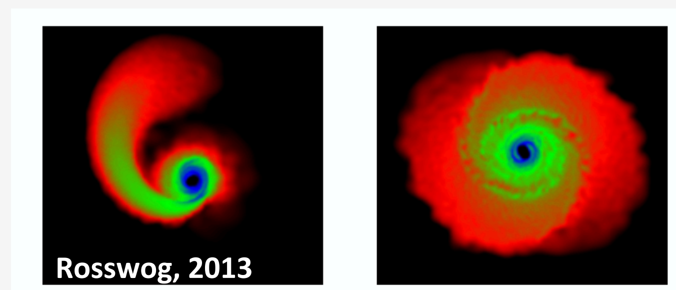

NS-NS and NS-BH inspiral and merger

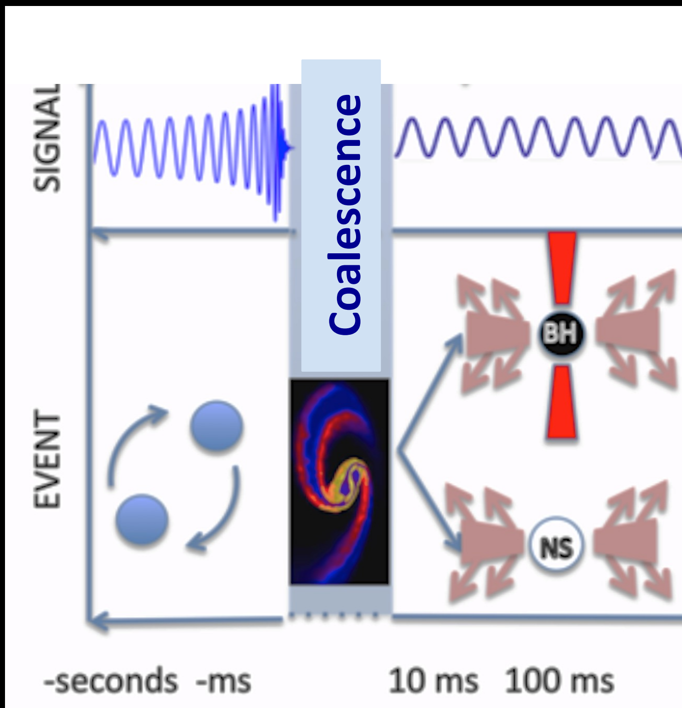

Dynamical Phase

Accretion phase

Fernandez & Metzger 2016, ARNPS, 66

The merger gives rise to:

- dynamically ejected unbound mass
- ejected mass gravitationally bound to the central remnant either falls back or circularizes into an accretion disk

NS-BH binary → unbound mass up to 0.1 Mo depends on **ratio of the tidal disruption radius to the innermost stable circular orbit**

If < 1 → NS swallowed by the BH no mass ejection

If > 1 NS → tidally disrupted, long spiral arms

which depends on **the mass ratio, the BH spin and the NS compactness**

See Kawaguchi et al. 2016,ApJ, 825, 52

NSBH COALESCENCE

- Before the merger, the BH is described by its mass M_{BH} and spin χ_{BH} which determine the radius of the ISCO, R_{ISCO}

- Once the NS approaches the BH, the tidal forces increase. The objects' internal structure become important as the orbital separation approaches the size of the bodies

- IF $d_{tidal} < R_{ISCO}$ ⇒ NS direct plunge into BH
  → little or no mass left outside of the BH
  → **NO EM COUNTERPART**

- IF $d_{tidal} > R_{ISCO}$ ⇒ NS effectively disrupted
  → BH remnant surrounded by baryon matter
  → **EM COUNTERPARTS**

ISCO = innermost stable circular orbit of the BH, inside which no material have a stable circular orbit around the BH

For a non rotating Schwarzchild BH $$R_{ISCO} = 6GM_{BH} / c^2 = 3R_S$$

For a rotating BH the equatorial ISCO also depends on the spin angular momentum

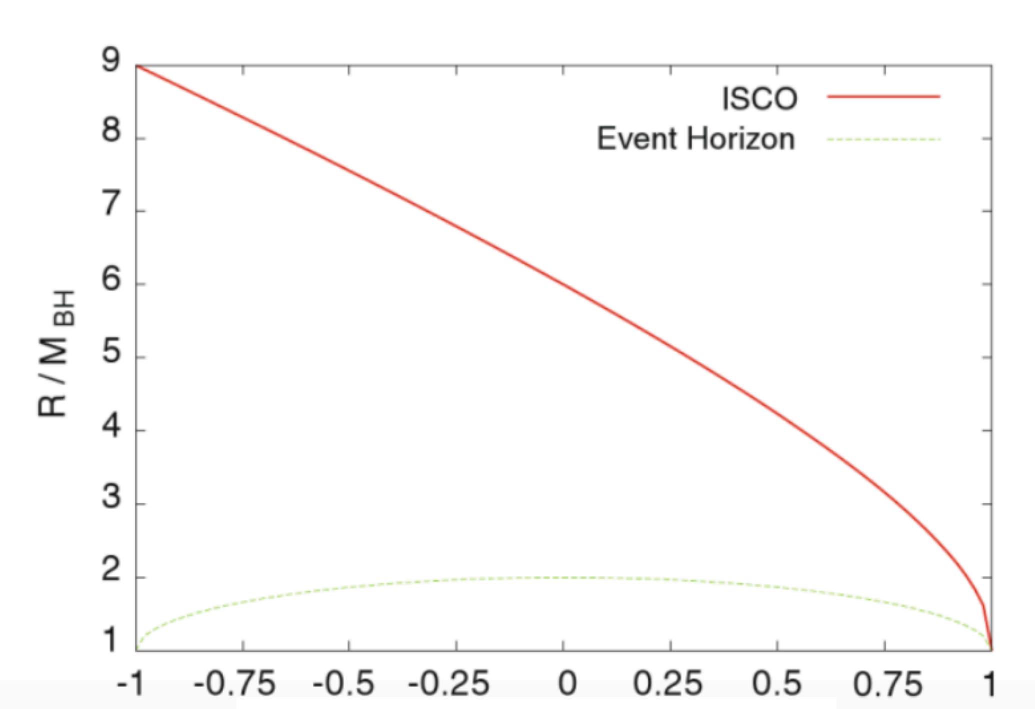

Kyutoku 2013

$$\chi_{BH} = cS / (GM_{BH}^2)$$ → Non dimensional spin parameter

$$\chi = cS/(GM_{BH}^2)$$ dimensionless spin parameter

- NS spin negligible → typically assumed $\chi_{NS} \sim 0$

NSs are expected to born rapidly rotating but before NSBH coalescence (which requires long time from their birth) they have time to spin down by dipole-emission (the lack of matter accreting onto the NS prevent spin-up by recycling)

- Assumed non-precessing binaries → BH spin vector aligned or anti- aligned with the orbital angular momentum

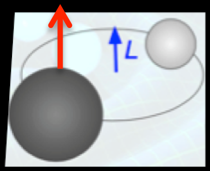

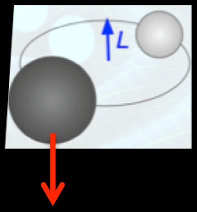

- Anti-aligned configurations → larger ISCO, favour direct plunge of the NS into the BH → no baryonic mass left outside the final BH to power an EM counterpart

Tidal disruption radius d_{tidal} radius at which tidal disruption occurs

The tidal disruption occurs when the tidal force of the BH is stronger than the self-gravity of the NS

$$\frac{M_{BH}}{r^3} R_{NS} \geq C^2 \frac{M_{NS}}{R_{NS}^2}$$

C=non dimensional coefficient
r =orbital separation

Newtonian theory

$$\frac{3M_{BH}}{d_{tidal}^3} R_{NS} \sim \frac{M_{NS}}{R_{NS}^2} \quad \Rightarrow \quad d_{tidal} \sim R_{NS} \left(\frac{3M_{BH}}{M_{NS}} \right)^{1/3}$$

Foucart et al. 2012

Foucart 2012

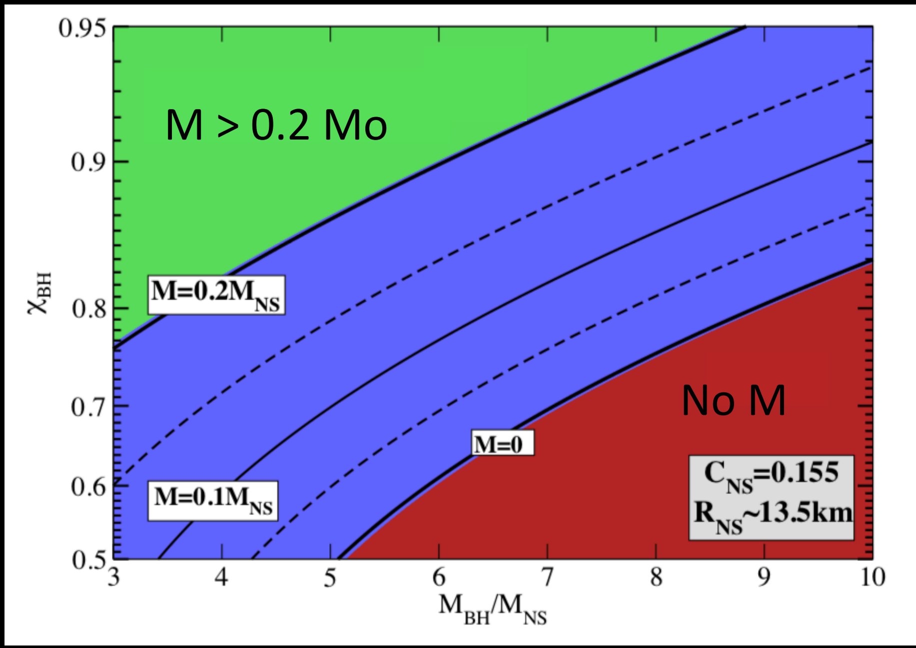

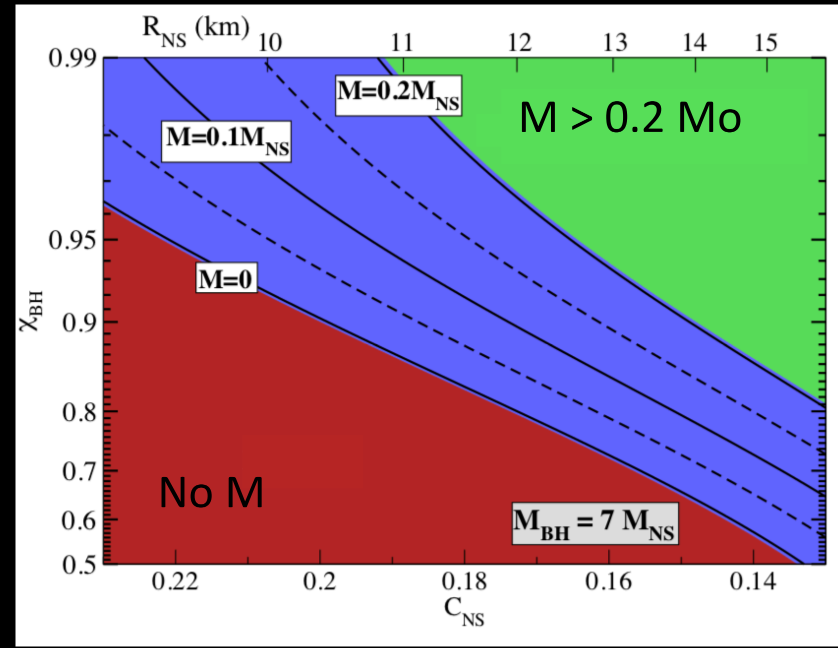

Large baryon mass left outside the merger remnant:

- Mass ratio BH/NS small → small BH mass
- Large BH spin angular momentum
- Small NS compactness

See Pannarale & Ohme 2014, Foucart et al. 2018, Barbieri et al. 2019

In the degenerate interiors of neutron stars EOS: $P \propto \rho^{\alpha}$

Small α → soft EOS (easier to compress)

High α → stiff EOS (harder to compress)

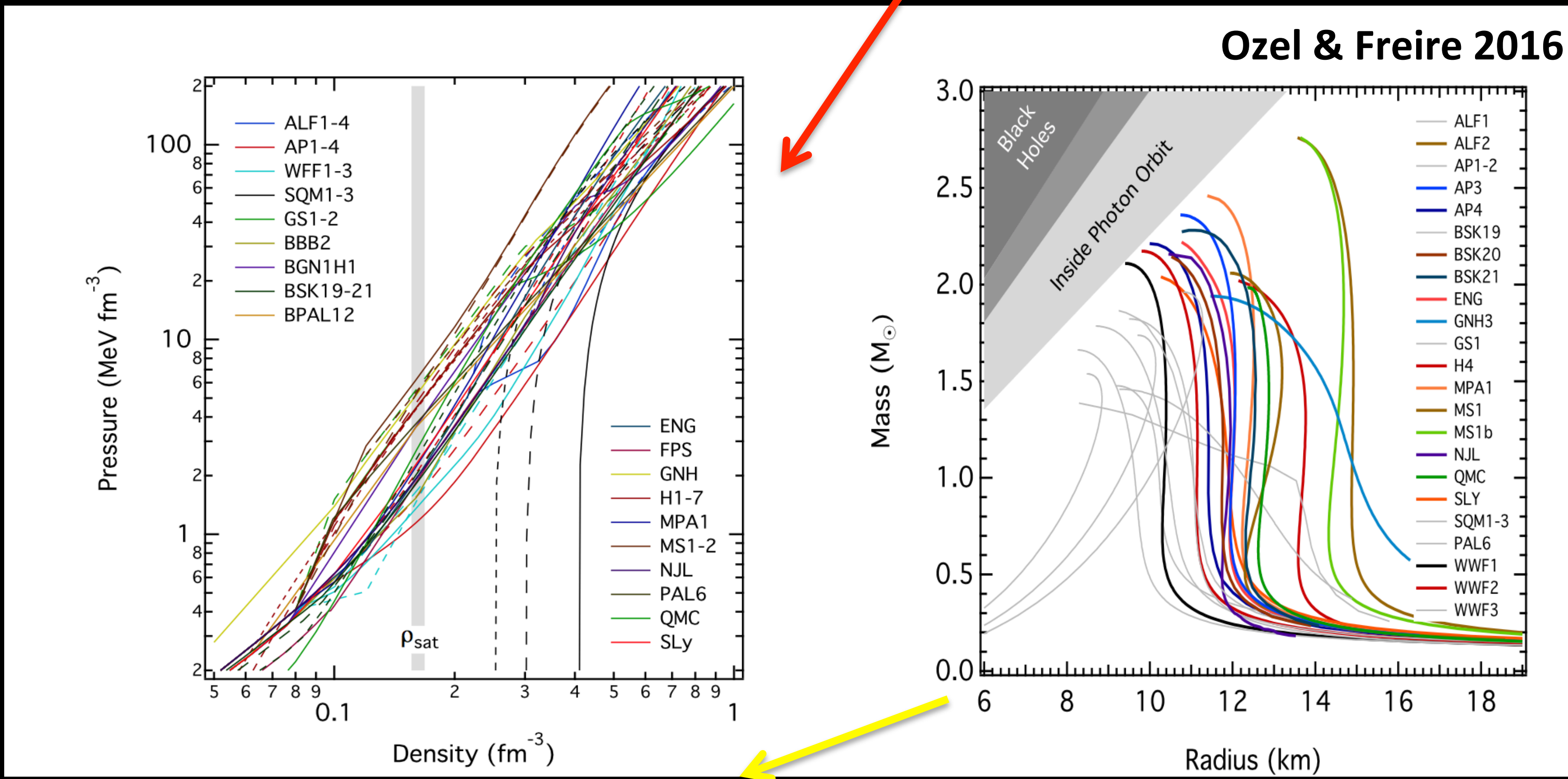

Mass-Radius relation is "unique" to the underlying EoS

- Soft EoS: low maximum M and smaller R for the same M (more compact)
- Stiff EoS: high maximum M and larger R for the same M (less compact)

In the degenerate interiors of neutron stars EOS: $P \propto \rho^{\alpha}$

Small α → soft EOS (easier to compress)

High α → stiff EOS (harder to compress)

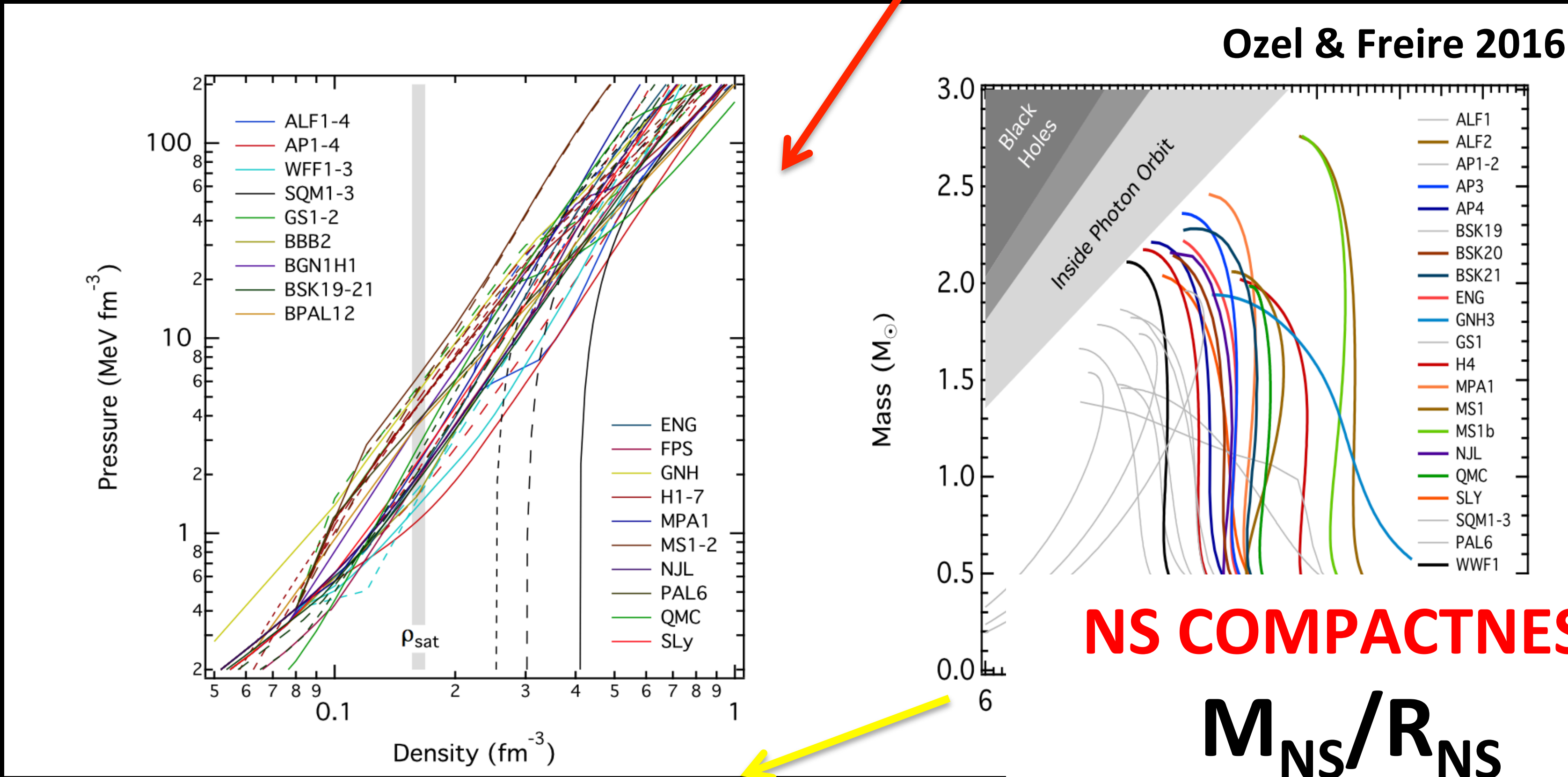

NS COMPACTNESS

M_{NS}/R_{NS}

Mass-Radius relation is "unique" to the underlying EoS

- Soft EoS: low maximum M and smaller R for the same M (more compact)
- Stiff EoS: high maximum M and larger R for the same M (less compact)

Foucart 2012

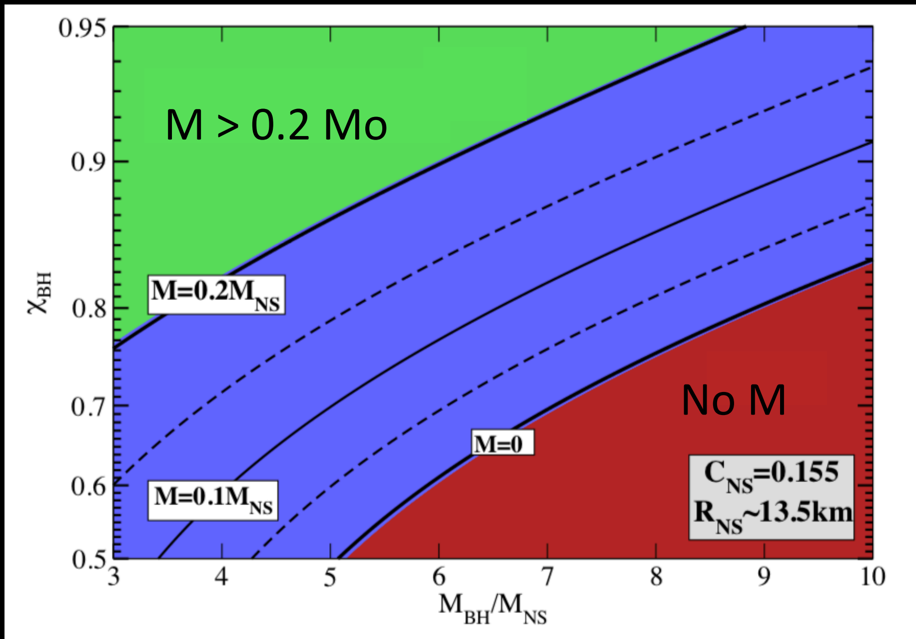

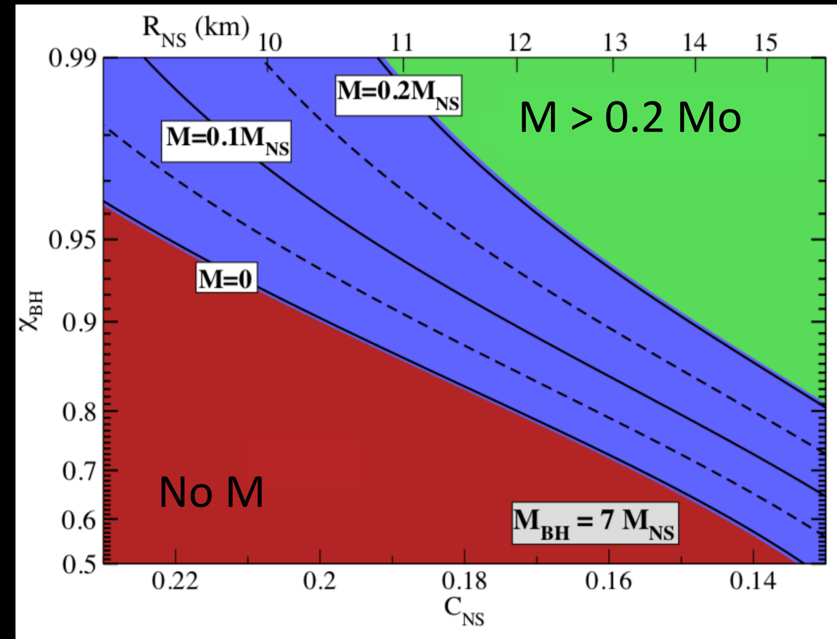

Large baryon mass left outside the merger remnant:

- Mass ratio BH/NS small → small BH mass
- Large BH spin angular momentum
- Small NS compactness → same M large NS radius, stiff EOS
  (harder to compress, easier to be disrupted)

See Pannarale & Ohme 2014, Foucart et al. 2018, Barbieri et al. 2019

NS-NS and NS-BH inspiral and merger

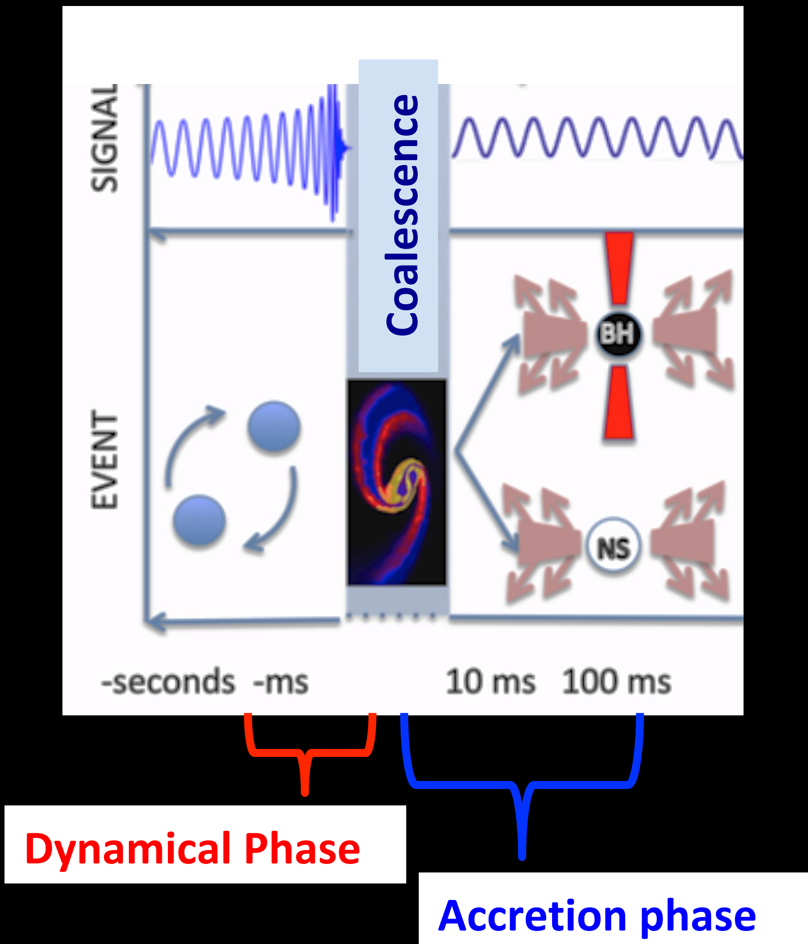

Fernandez & Metzger 2016, ARNPS, 66

- Ejected material gravitationally bound from the central remnant can fall back or circularizes into an accretion disk

Disk mass up to ~ **0.3Mo**
Disk mass depends on the **mass ratio of the binary, the spins of the binary components, the EOS, and the total mass of the binary**

For NS-BH see e.g. Foucart 2012, PhRvD, 86;
Maselli & Ferrari, PhRvD, 89;
Pannarale & Ohme, ApJL, 791

Outflow mass and geometry influence the EM emission

Central remnant of NS-NS or NS-BH merger

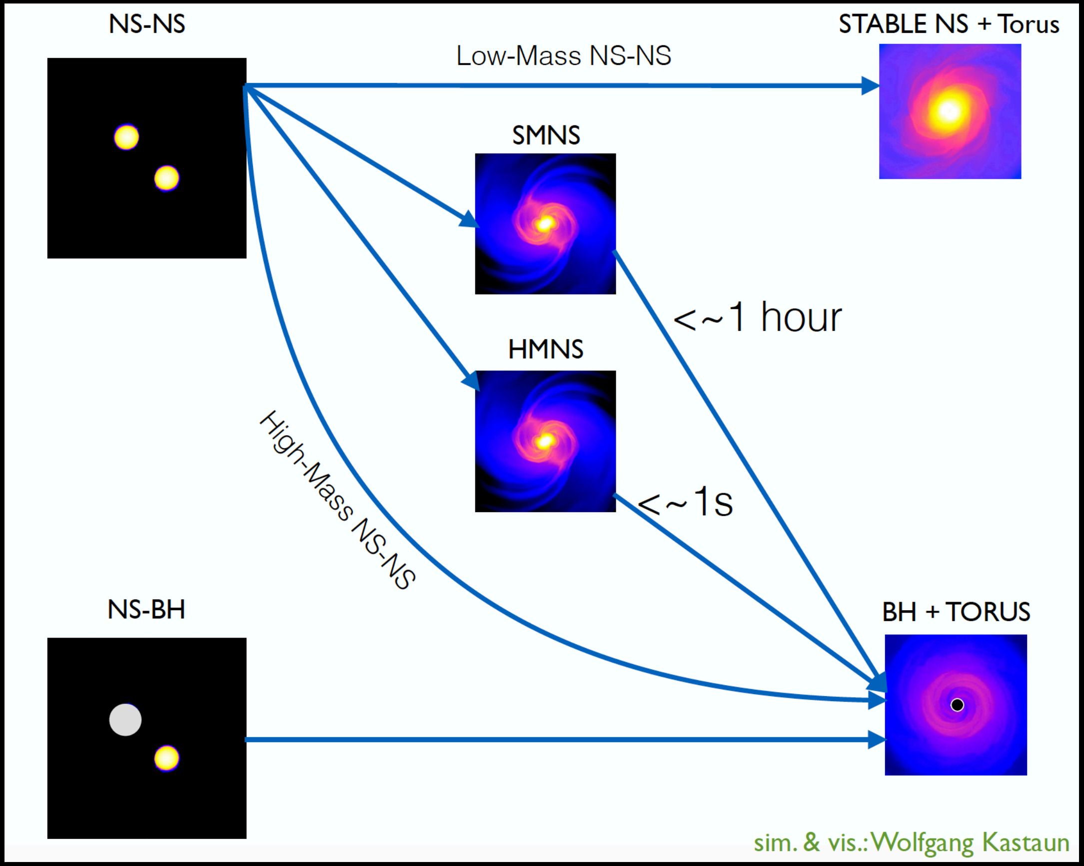

The central remnant influences GW and EM emission

What is central remnant?

- It depends on the total mass of the binary
- The mass threshold above which a BH forms directly depends on EOS

EM non-thermal emission

Gamma-Ray Bursts

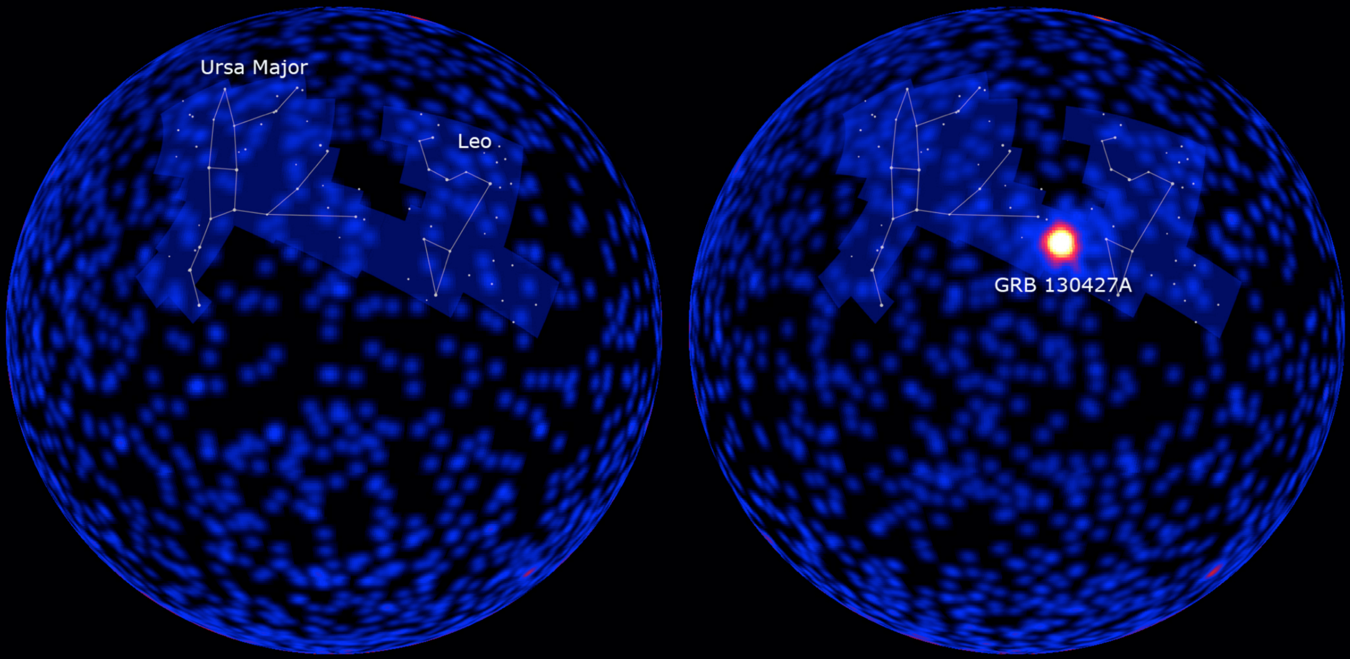

Before and after Fermi LAT observation of GRB 130427A

Brief, sudden, intense flashes of gamma ray radiation which release energy up to **~ 10^{53} erg** (isotropic-equivalent)

Duration: **from few ms to hundreds of s**
Observational band: **10 keV – 1 MeV**
Flux: **10^{-8} - 10^{-4} erg cm^{-2} s^{-1}**

GRBs were discovered serendipitously in the late 1960s by U.S. military satellites looking out for Soviet nuclear testing

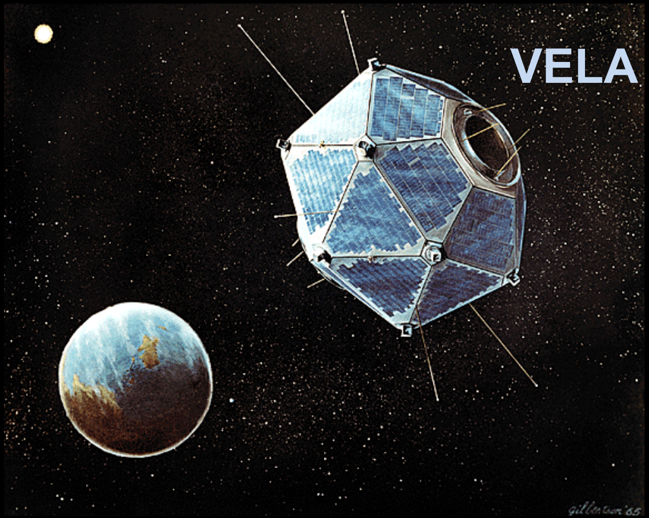

Galactic or cosmological?

BATSE
20 keV-MeV
(1991-2000)

Isotropic angular distribution

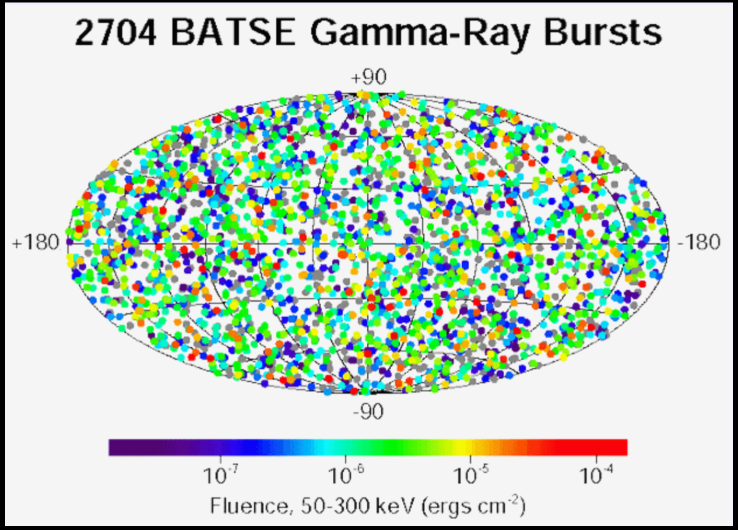

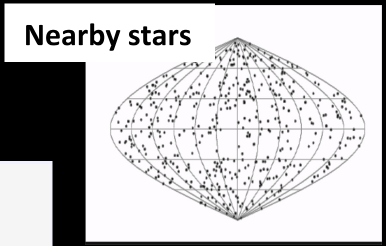

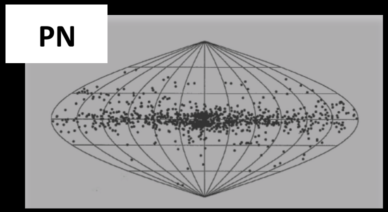

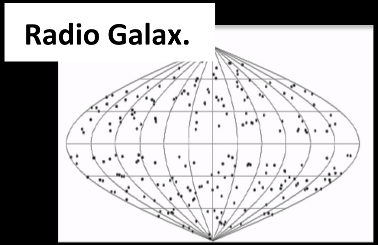

Paczynsky, PASP, 107, 1167

BeppoSAX

(1996-2002)

Italian–Dutch satellite for X-ray astronomy resolved the origin of gamma-ray bursts

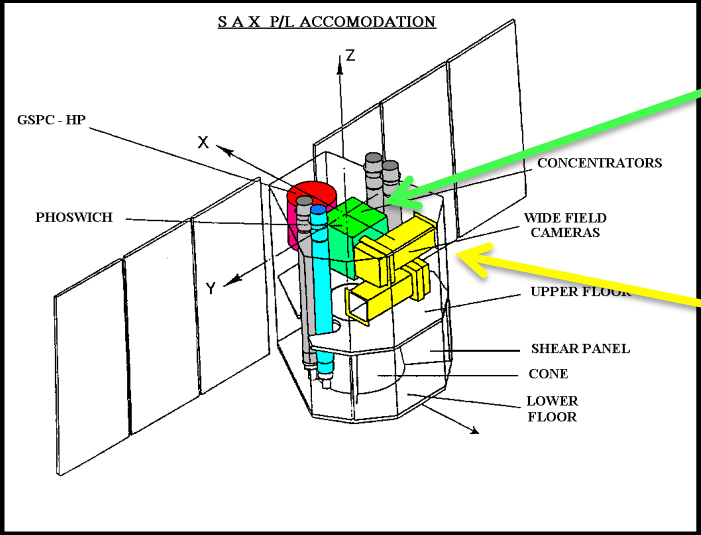

Scintillator for gamma-rays
60-600 keV, poor angular resolution

Wide Field Camera (WFC)
2-30 keV; 20x20 degree FoV
5 arcmin angular resolution

GRB 970228 in the FOV of the WFC

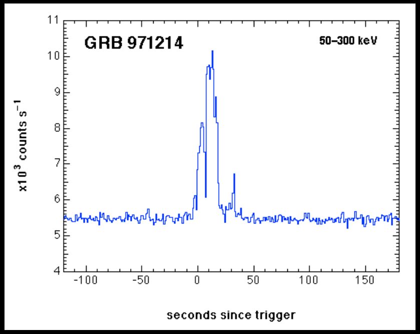

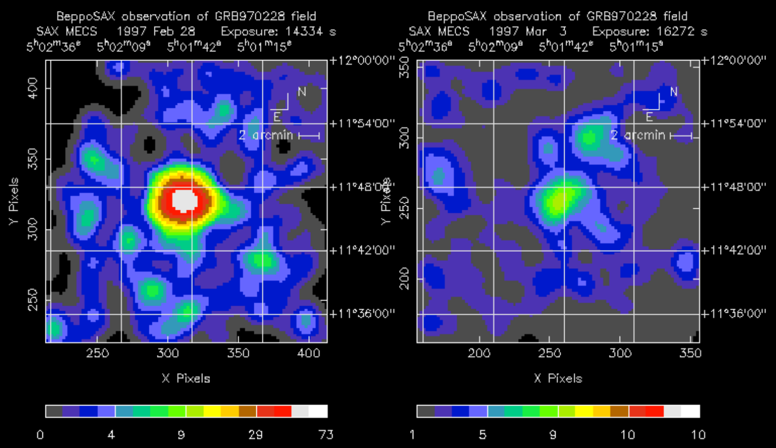

Well localized fading X-ray afterglow!

Costa et al., 1997

Optical afterglow/host galaxy

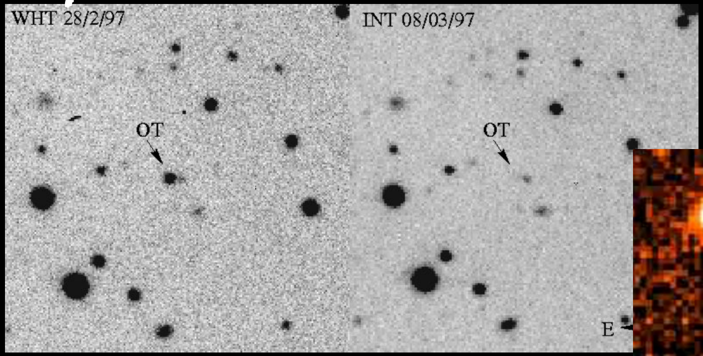

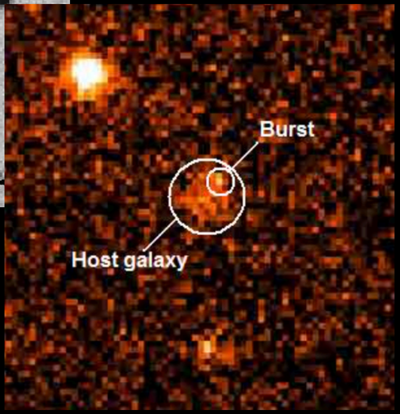

z=0.695, D_L=3.6 Gpc

Cosmological redshift

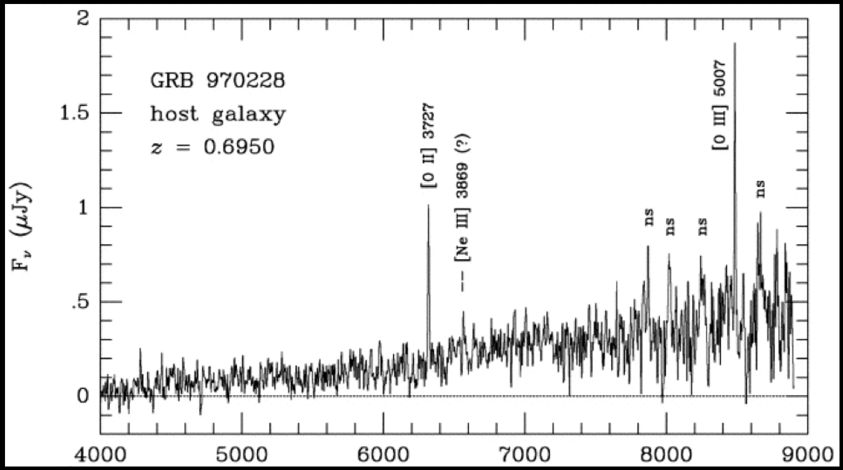

Groot, Galama, van Paradijs, et al IAUC 6584, March 12, 1997

van Paradijs et al., 1997

Swift: "everything in space"

Since Nov. 2004

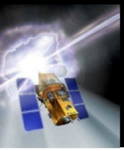

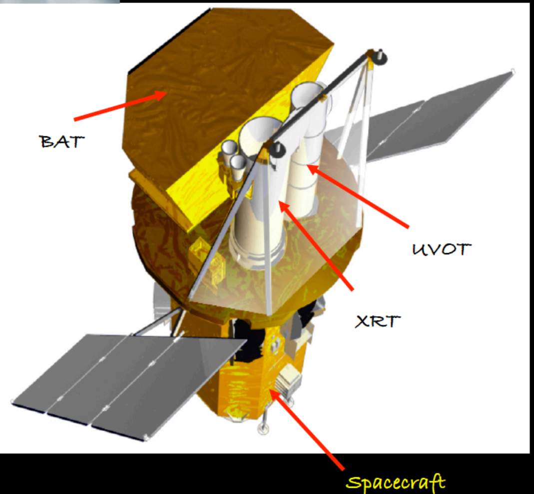

Satellite slews (1 min) and repoints its X ray (XRT) and UV telescopes to observe the error region of the GRB.

T<10 sec
θ< 4′
E>15 kev

T<100 sec
θ < 5″
E<10 kev

T<300 sec
Optical/NIR

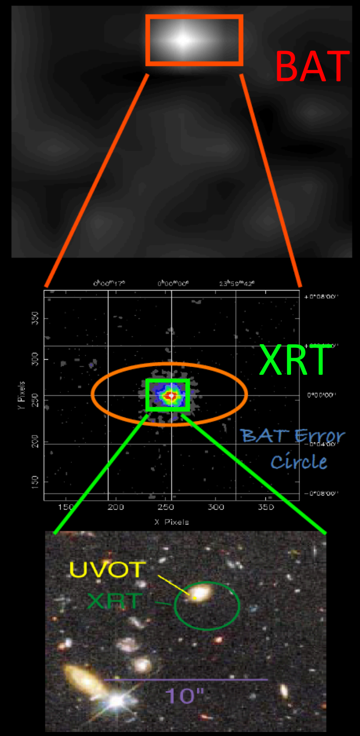

GRBs are extragalctic, cosmological, and occur in galaxies

GRBs host galaxies observed by HST

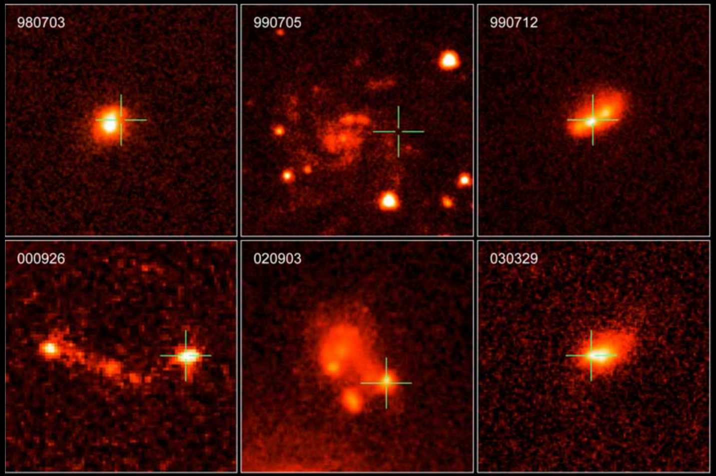

GRB progenitors

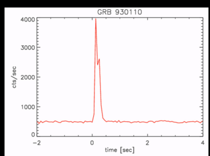

Bimodal duration distribution

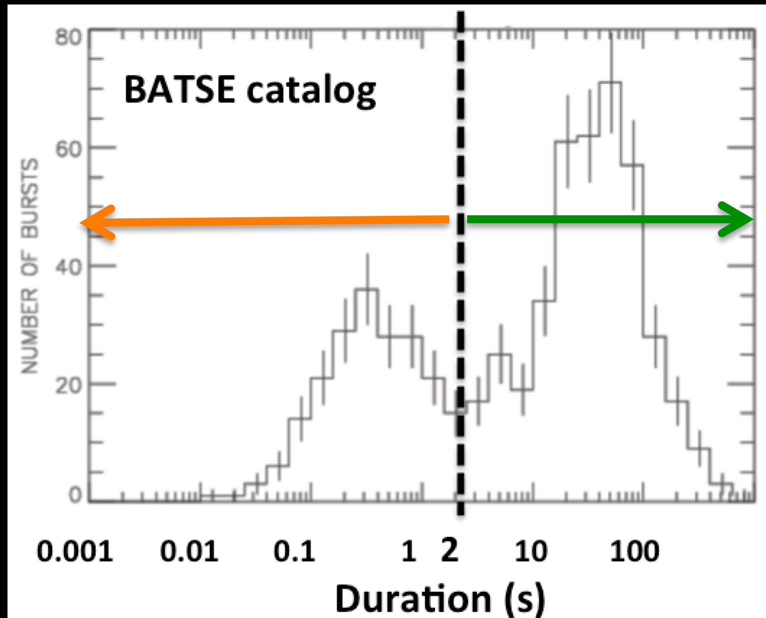

Kouveliotou et al. 1993

Hardness ratio

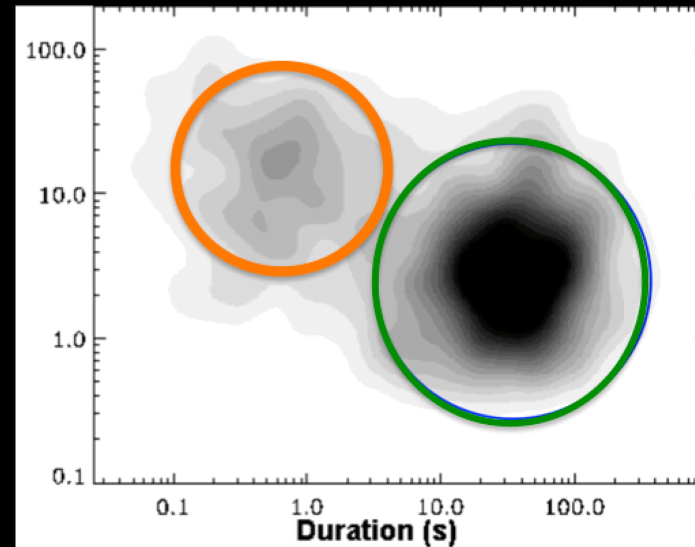

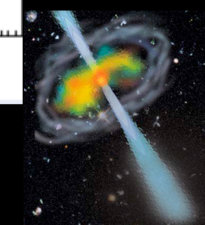

Different Progenitor

Short Hard GRB

- lack of observed SN
- association with older stellar population
- larger distance from the host galaxy center (~ 5-10 kpc)
- accretion timescale of disk in binary merger model is short (t ~ 1s)

➡ **NS-NS NS-BH mergers**

Long Soft GRB

- observed Type Ic SN spectrum
- accretion disk is fed by fallback of SN material onto disk, timescale t ~ 10-100s

➡ **Core-collapse of massive stars**

Long GRB and Supernovae

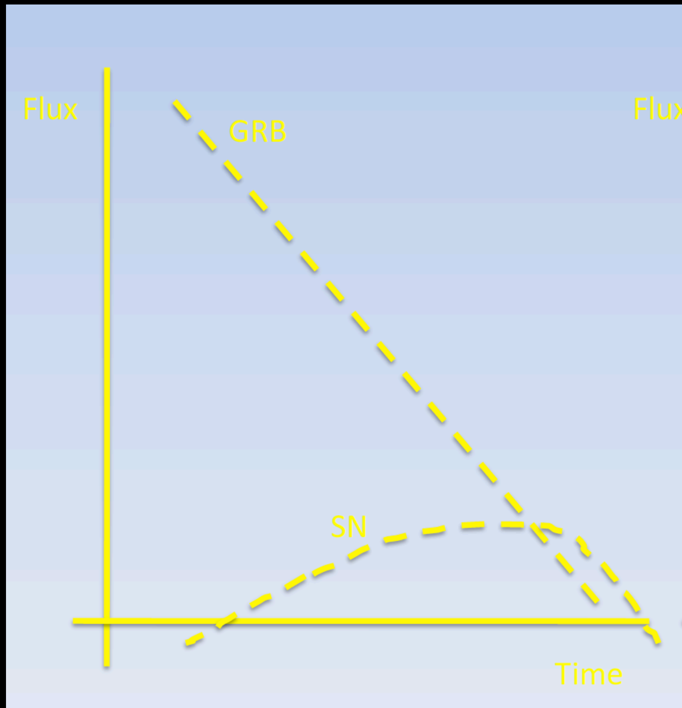

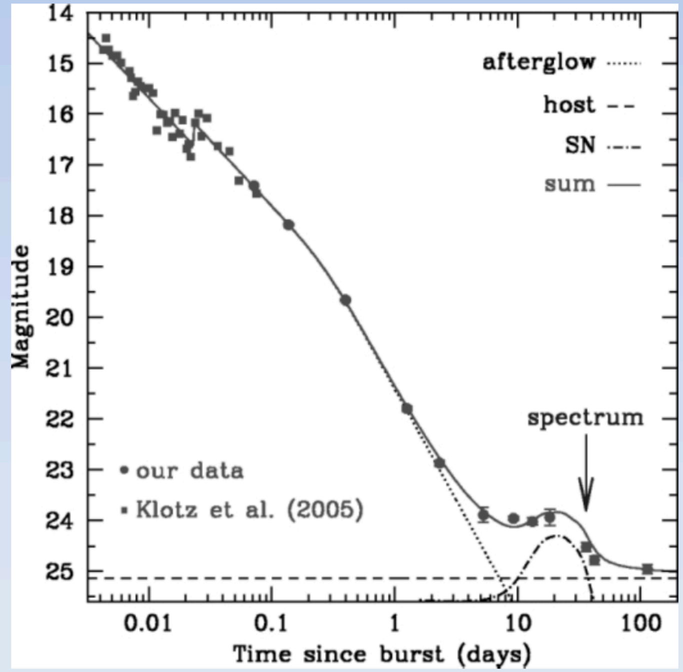

Galama et al. 1998; Stanek et al. 2003; Hjorth et al. 2003; Della Valle et al. 2003; Malesani et al. 2004; Soderberg et al. 2005; Pian et al. 2006; Campana et al. 2006; Della Valle et al. 2006, Bufano et al. 2012, Melandri et al. 2012, Schulze et al. 2014, Melnadri et al. 2014 and others…

SN 1998bw/GRB 980425
Type Ic supernova

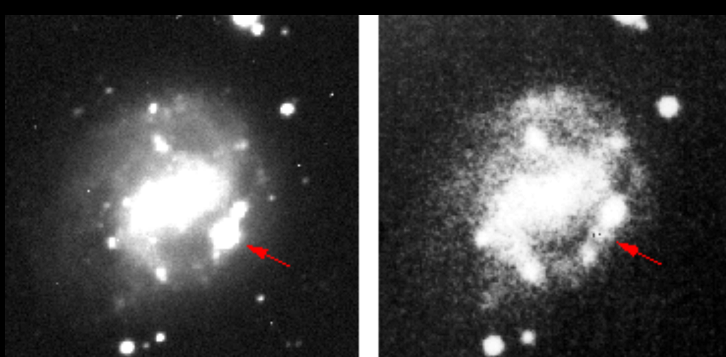

Iwamoto et al 1998; Woosley et al. 1999

Spectra

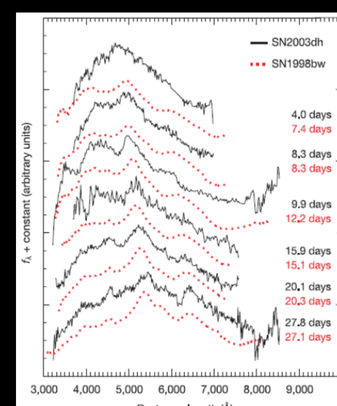

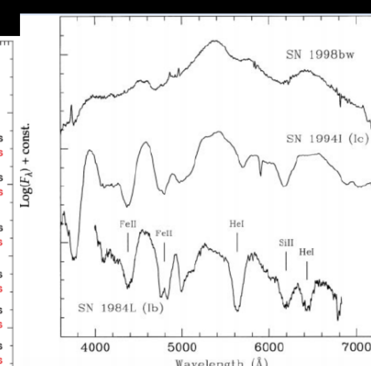

GRB EMISSION

Image Credit: ESA/Hubble, M. Kornmesse

Prompt emission phase:

Energy range: keV-MeV

Variability time-scales: ms-s

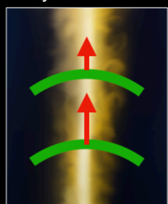

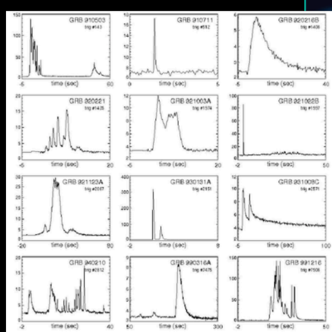

Shemi & Piran (1990)

Rees & Meszaros (1994)

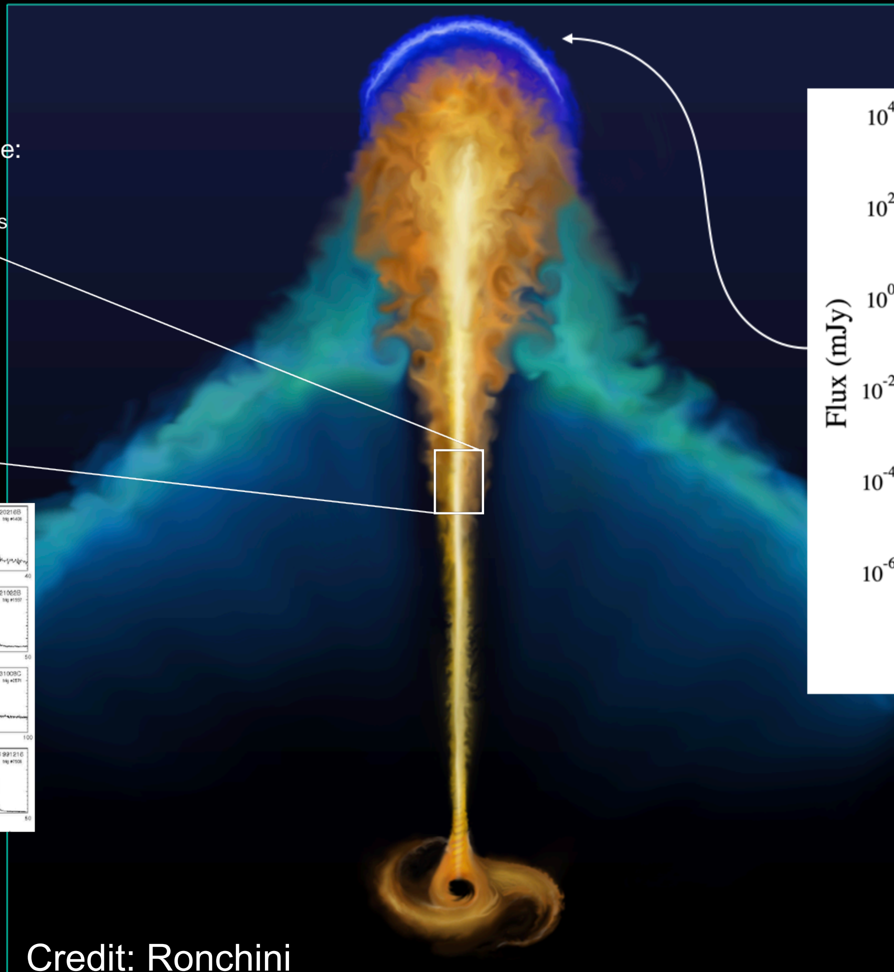

Afterglow phase

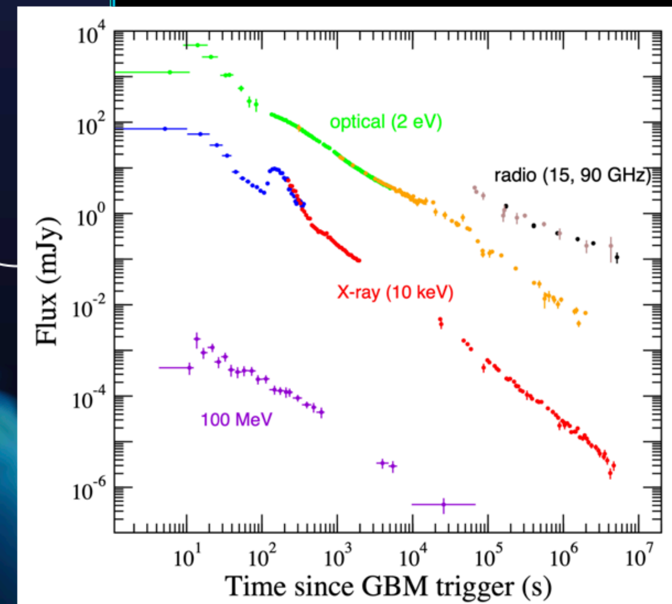

From Panaitescu et al (2013)

GRBs emission - Fireball Model

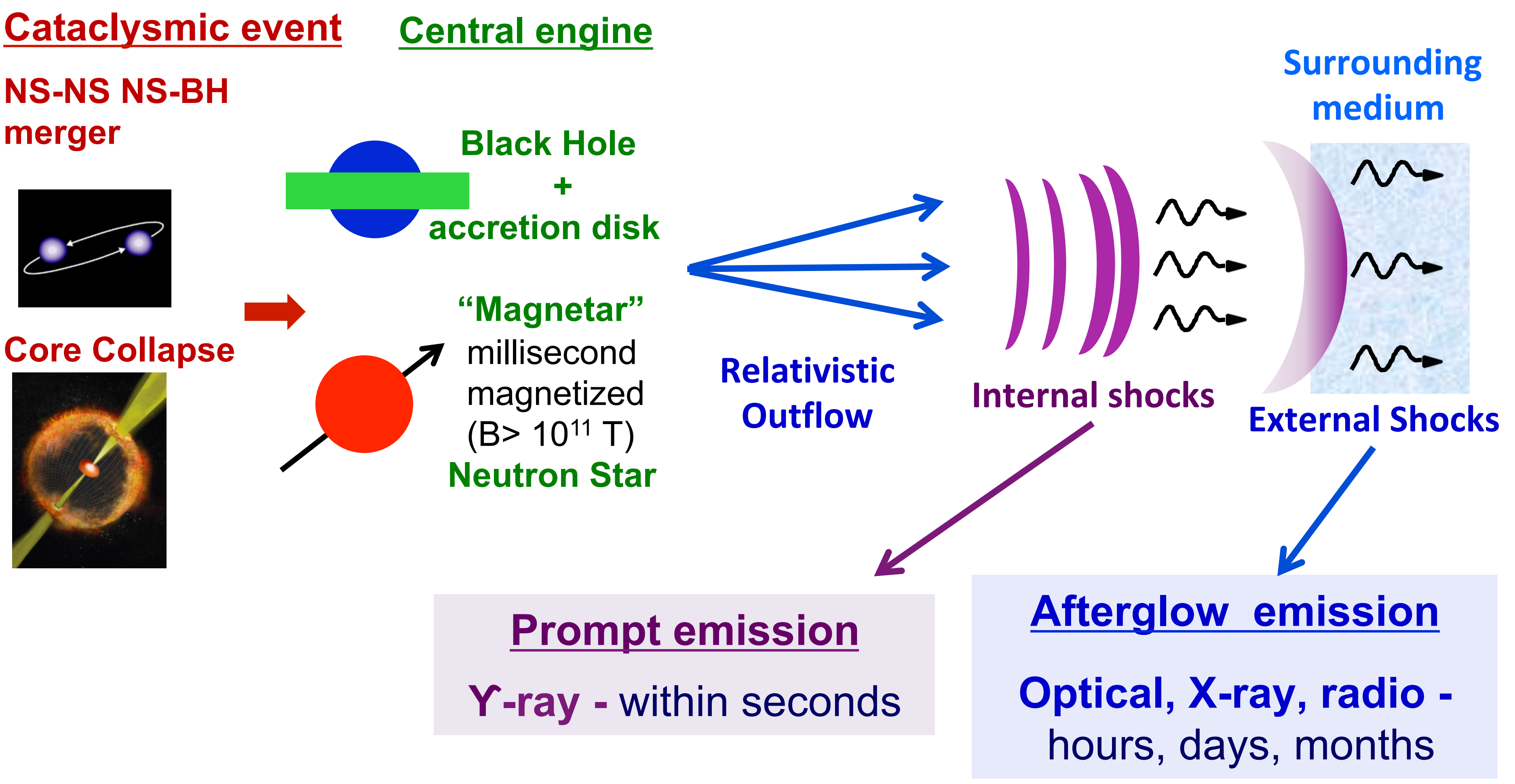

Kinetic energy of the relativistic jet converted into radiation

Mjet = 10^{-7}-10^{-5} Mo, $\Gamma \geq 100$, E=10^{48}-10^{51} erg

Optical afterglows of on-axis GRBs

On-axis GRBs

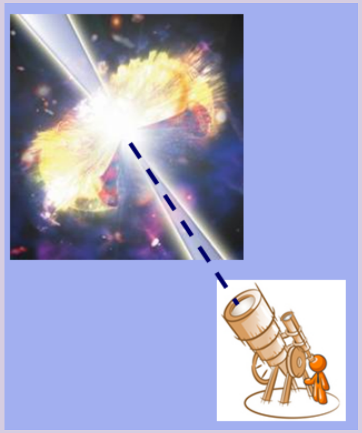

Observed GRB optical afterglows

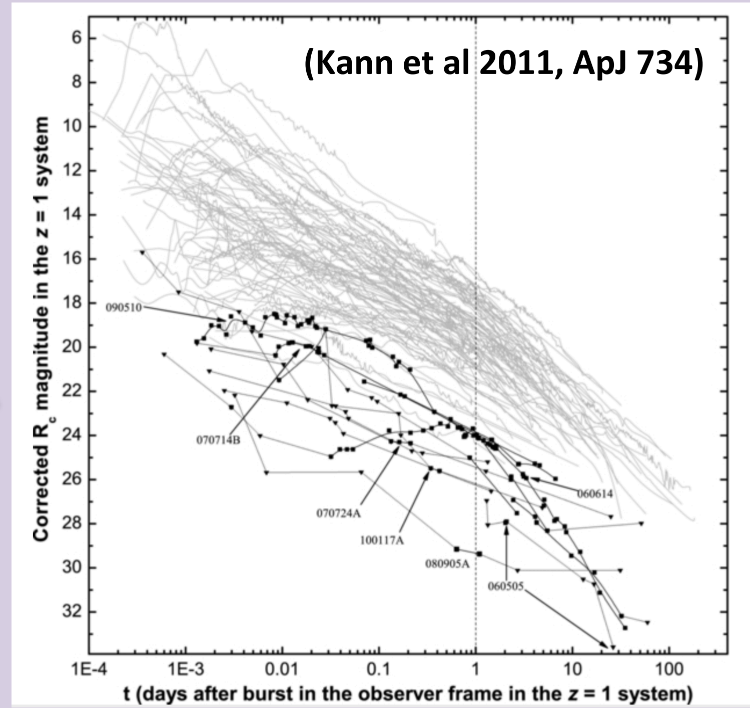

Source at 200 Mpc

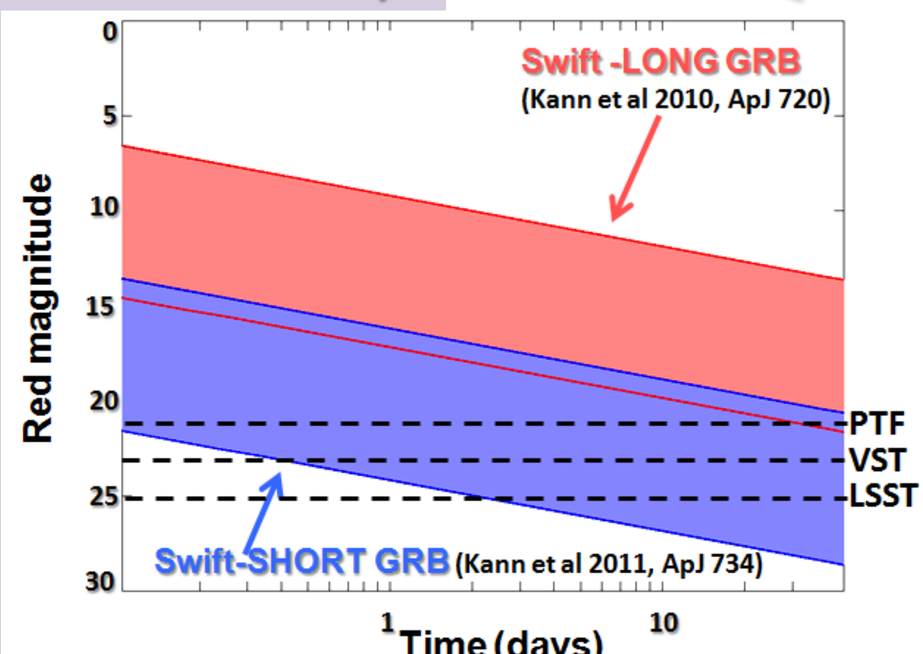

On average the optical afterglow decays as a **power law** $\mathbf{time^{-\alpha}}$ with **α in the range 1 to 1.5**

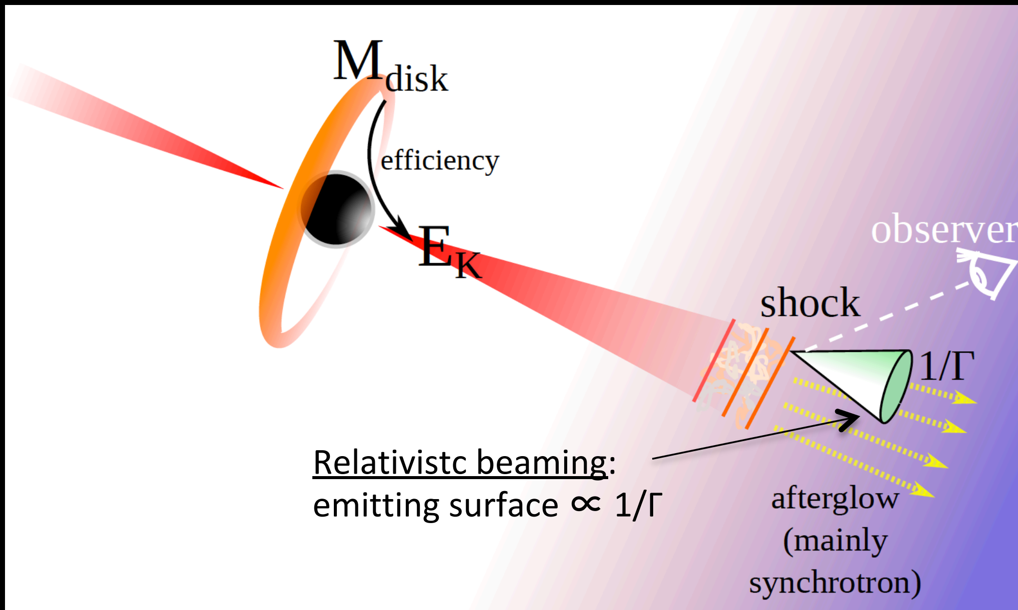

Relativistic beaming angle

$$\theta_b \propto 1/\Gamma$$

(within which ejecta radiates) increases due to the ejecta deceleration

$$\Gamma = \frac{1}{\sqrt{1-\beta^2}} \qquad \beta = \frac{v}{c}$$

Early EM emission detectable only by on-axis observers

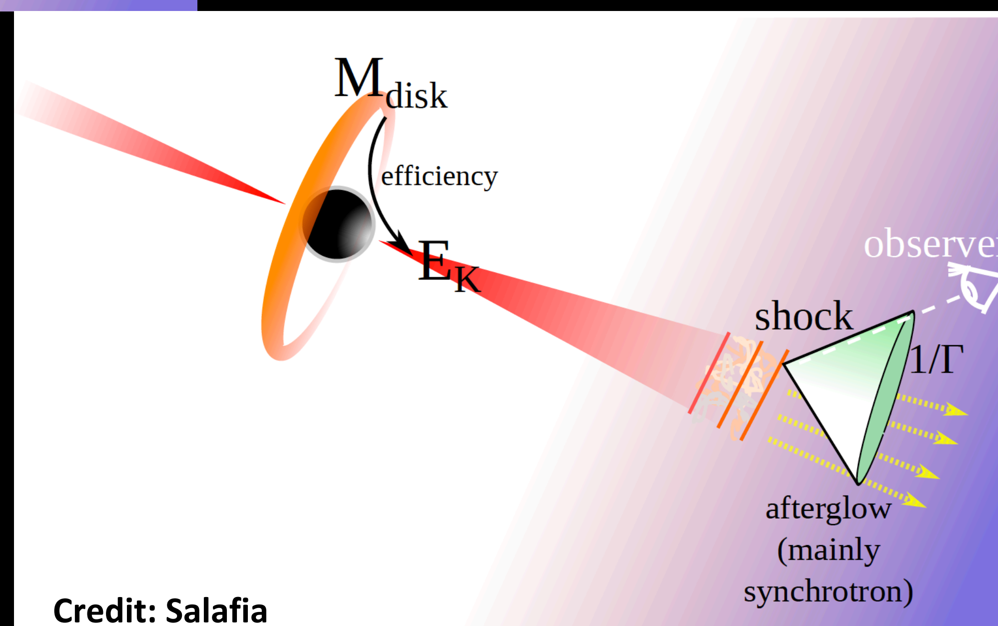

Credit: Salafia

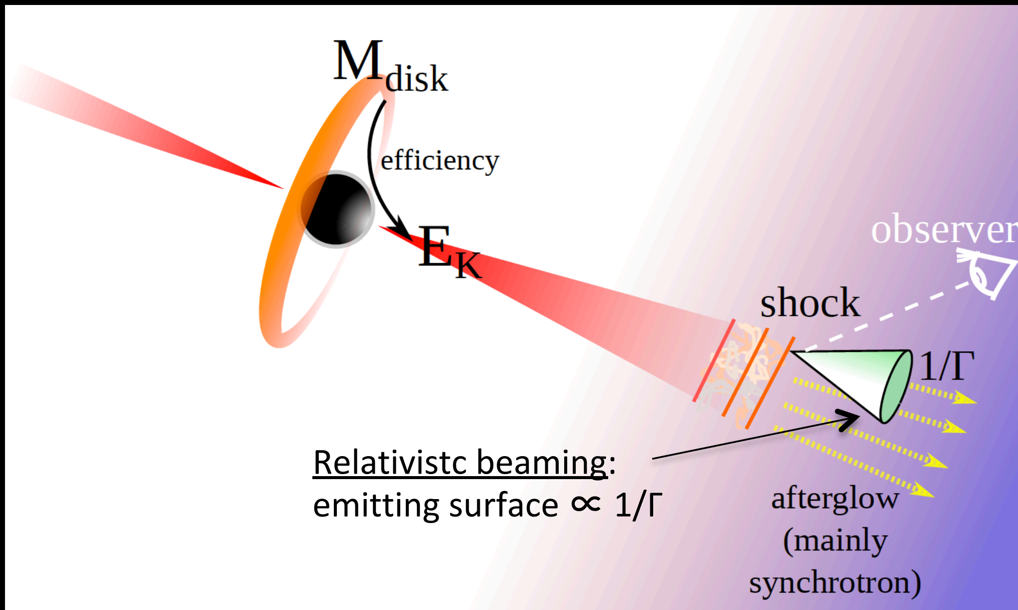

Early EM emission detectable only by on-axis observers

EM emission detectable also by off-axis observers

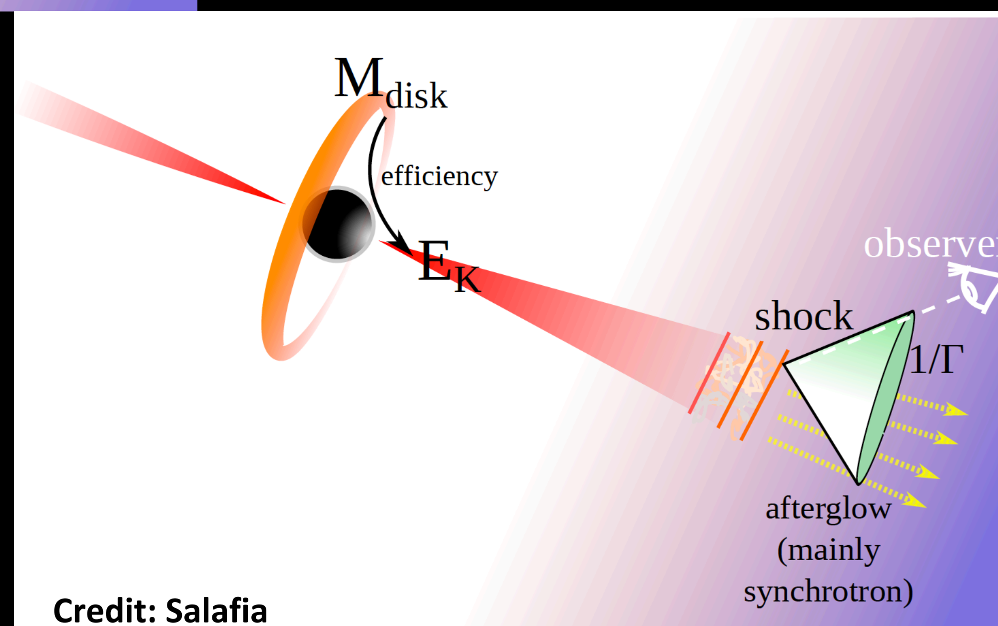

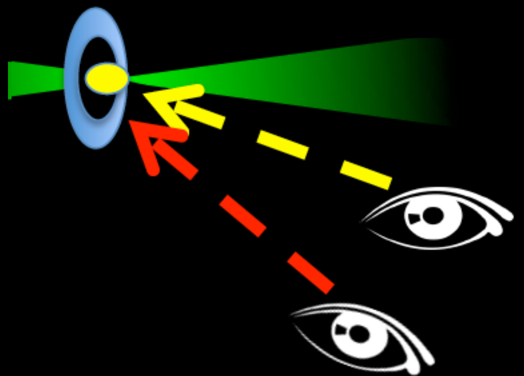

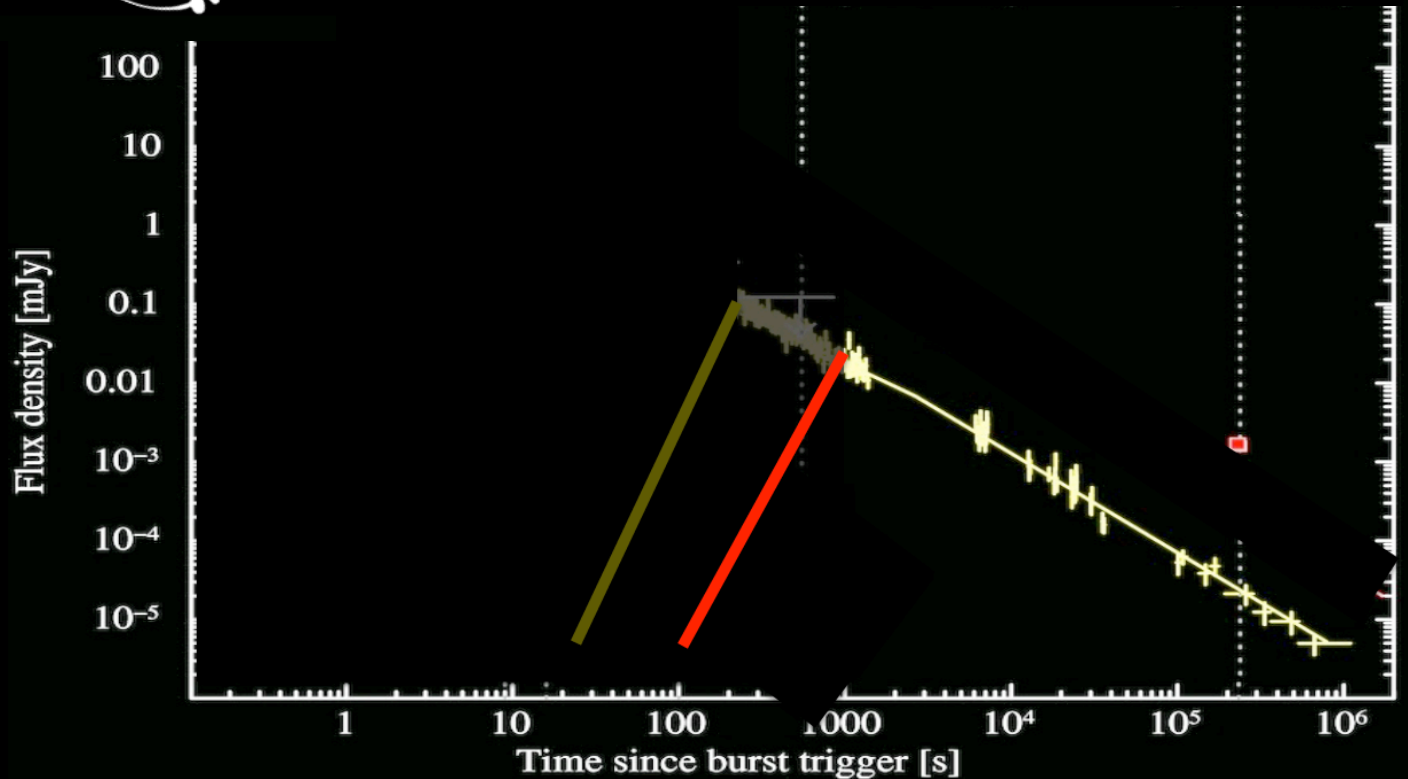

Credit: Ghirlanda

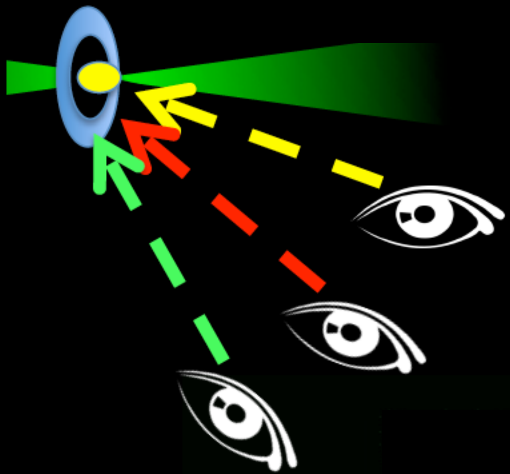

More off—axis:
(a) the emission peaks later
(b) the flux at peak is fainter

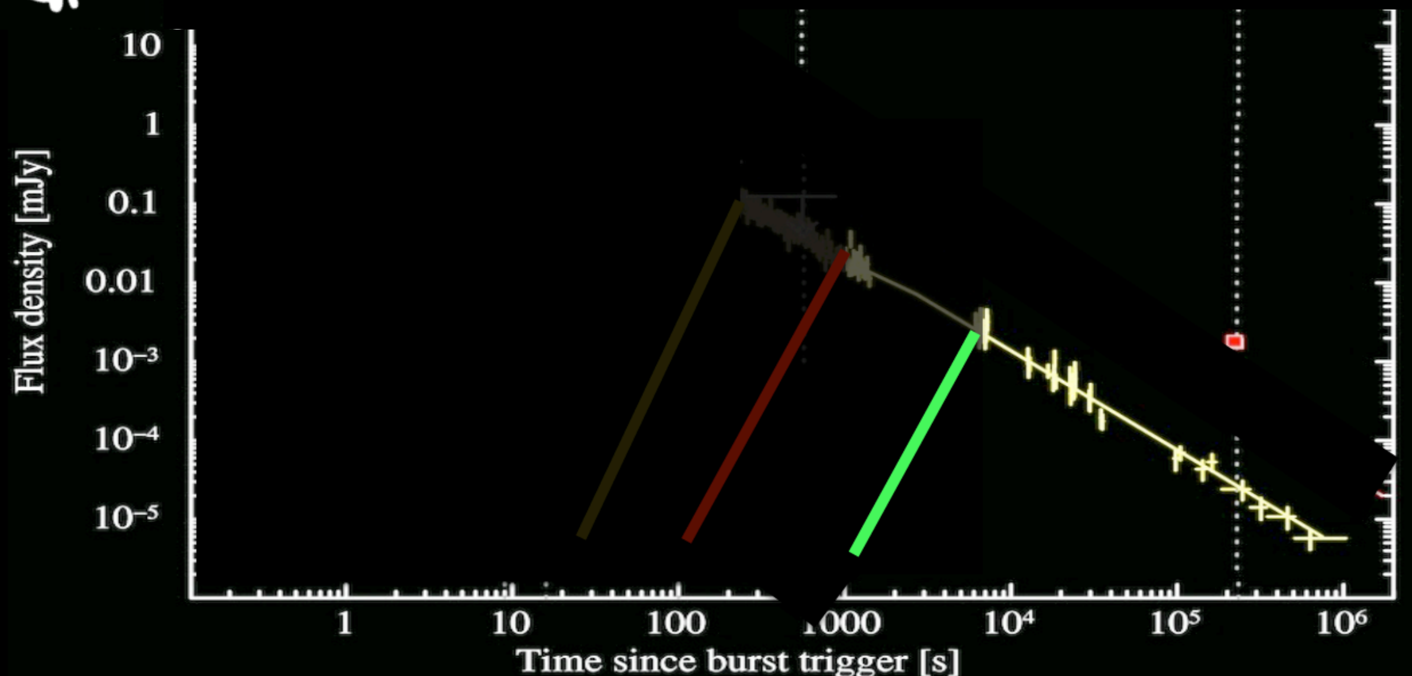

Credit: Ghirlanda

Optical afterglows of Off-axis GRBs

Off-axis GRB

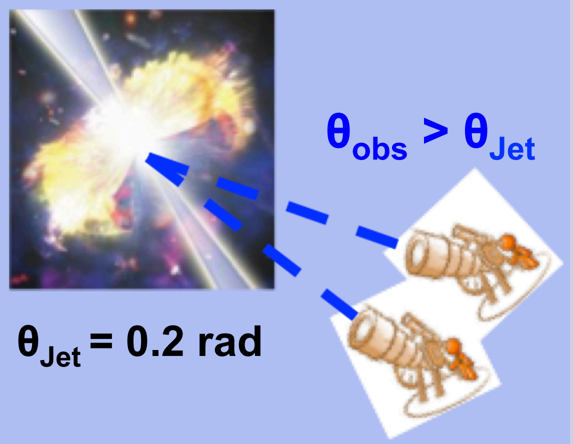

θ_{Jet} = 0.2 rad

Modelled afterglows - Source at 200 Mpc

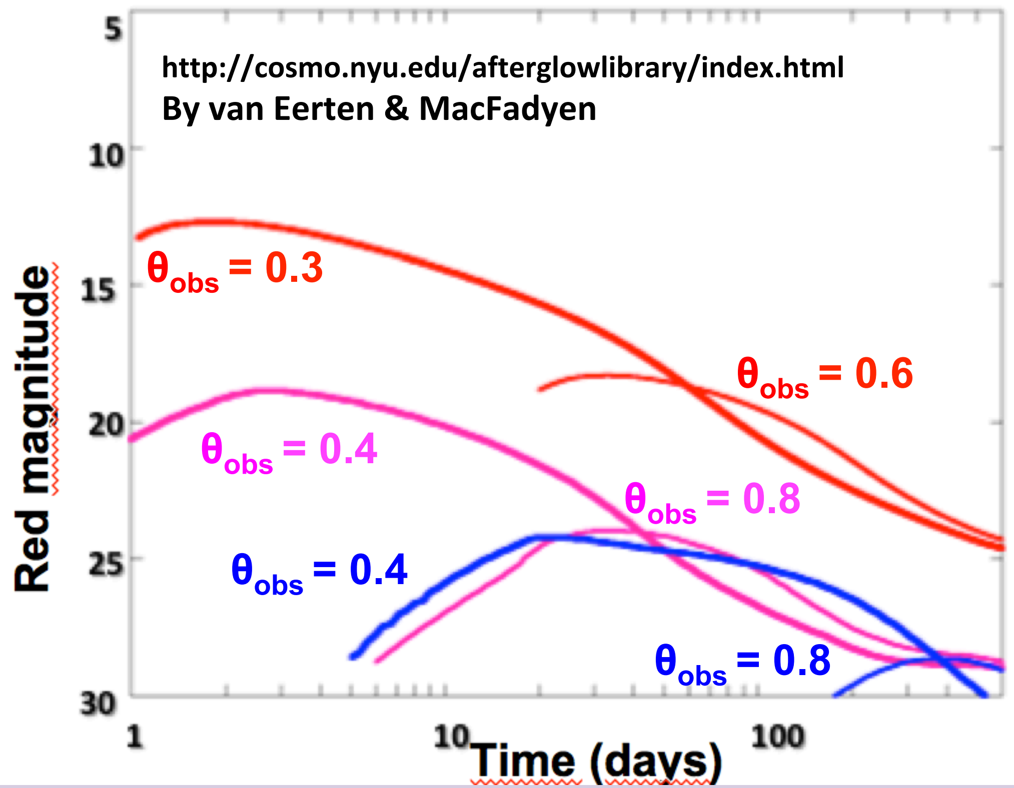

LONG bright GRB

E_jet = 2e51 erg, n = 1 cm^{-3}

LONG faint/ SHORT bright GRB

E_jet = 1e50 erg , n=1 cm-3

SHORT GRB

E_jet = 1e50 erg , n=10^{-3} cm^{-3}

Short GRB afterglows in numbers

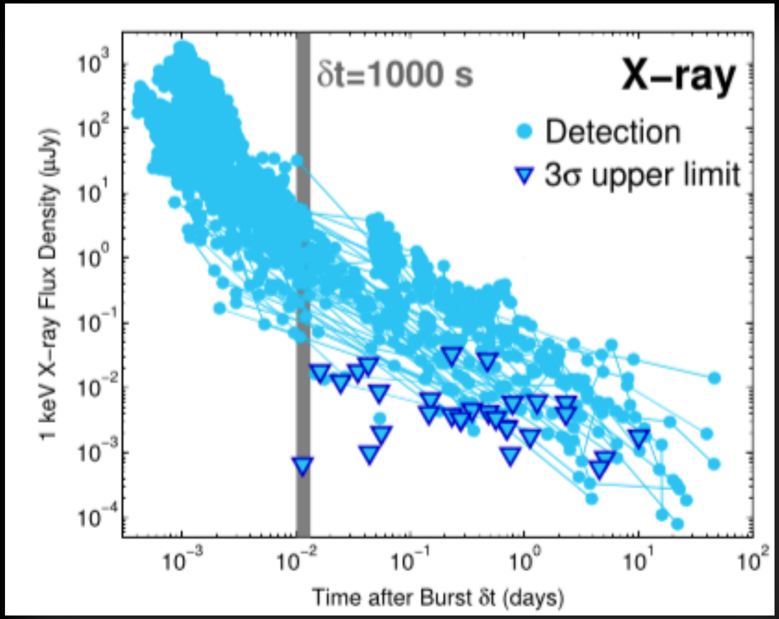

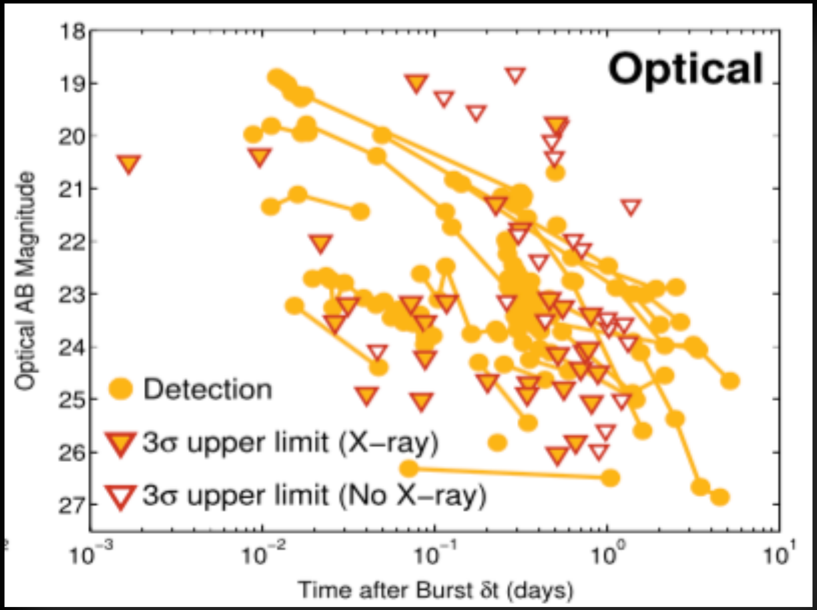

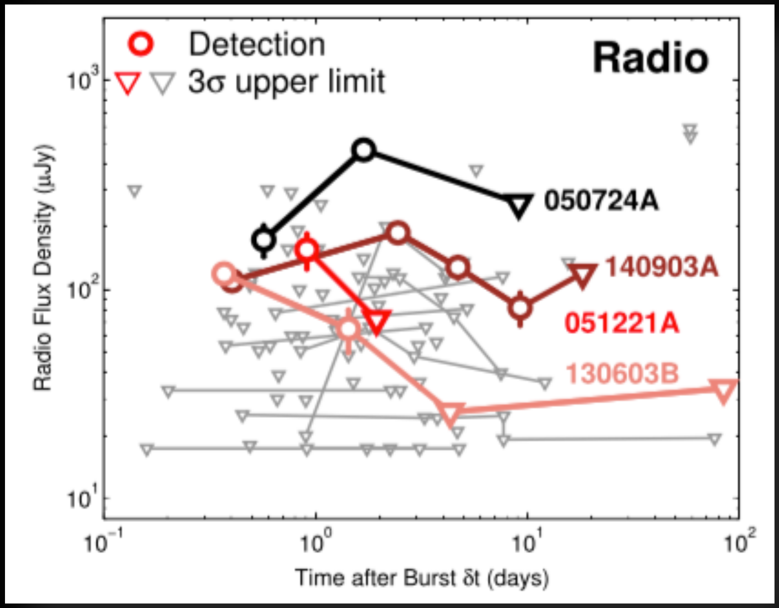

- About 140 SGRBs detected since 2005
- Afterglow detection percentage :
  - 90% in X-rays
  - 40% in opt
  - 7% in radio
- About 30 with redshift
- z_{min}=0.12 → 560 Mpc
- Energy =10^{48-52} erg

Fong et al. 2015

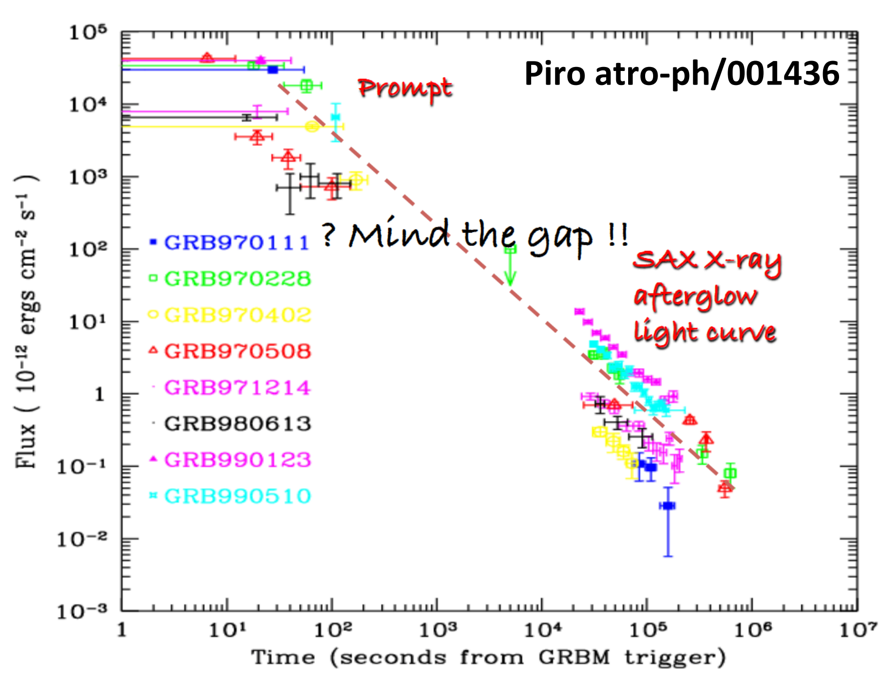

X-ray afterglow before Swift

X-ray afterglow NOW

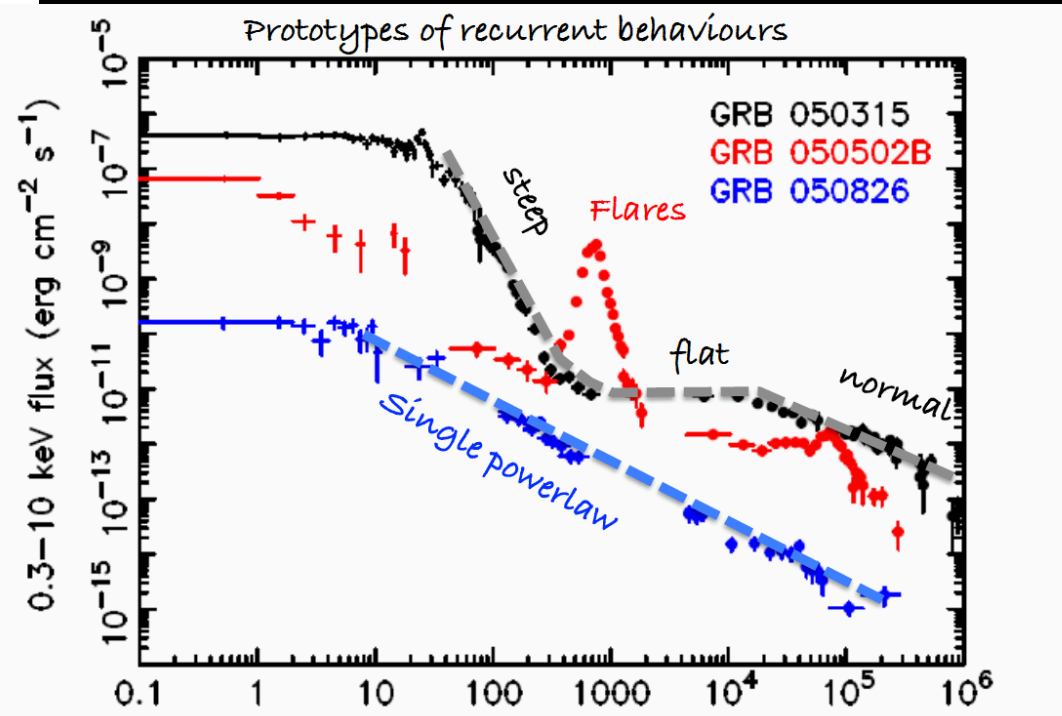

Gerhels et al. 2010